F-PM-1S PRIMARY PHOTOPHYSICAL AND PHOTOCHEMICAL PROCESSES IN VISUAL TRANSDUCTION. Aaron Lewis, School of Applied and Engineering Physics, Cornell University, Ithaca, NY 14853

Several experiments suggest that energy is stored in the primary photonic event in visual transduction. A crucial test of this hypothesis is that bathorhodopsin can thermally revert in certain cases to rhodopsin. For example, bathoiodopsin and bathobacteriorhodopsin have thermal pathways back to iodopsin and bacteriorhodopsin. A cis-trans isomerization is not an energy storing process and, furthermore, experiments indicate that even though bacteriorhodopsin has spectral transitions which are similar to all rhodopsins, it does not involve a formal cis-trans isomerization. Resonance Raman spectroscopy is providing the first *in situ* structural information on the retinylidene chromophore. Our spectra indicate that the primary action of light is to delocalize e^- density out of the polyene portion of the retinylidene chromophore, thus inducing charge polarization and $\delta+$ charges on the tertiary centers at carbons 5, 9 and 13. However the Schiff base is still protonated in bathorhodopsin and curiously the e^- density in the $-C=\overset{+}{N}-$ bond is identical to rhodopsin even though the C=C bonds have significantly lower e^- density. A relocalization of e^- density occurs and the Schiff base is deprotonated by metarhodopsin II. The initial charge polarization can store part of the photon energy and then the positive centers at carbons 5, 9 and 13 appear to induce in msecs e^- replacement and subsequent ejection of the Schiff base H^+. Thus the cis-trans isomerization is not the crucial result of the photonic event. In fact, bacteriorhodopsin which is biologically an energy converter has evolved to convert light energy efficiently into an ejected H^+ without an endoenergetic isomerization. However photoreceptor rhodopsins are not primarily energy convertors but quantum detectors and thus must have irreversibility. This we believe is the biological role of the cis-trans isomerization while the role of the ejected H^+ appears to be tied to the energy transduction process.

F-PM-2S RESONANCE RAMAN SPECTROSCOPY OF HEMEPROTEINS. L. Rimai, Research Staff, Ford Motor Company, Dearborn, Mich. 48121

The general feature of the Resonance Raman Spectra of the heme chromophore in hemeproteins will be reviewed, with special emphasis on data obtained with excitation near the Soret band. The latter contains most of the information on the low frequency vibrations (below 400 cm^{-1}) which offer a more specific signature of specific liganded forms of particular proteins than the balance of the spectrum. Based on a discussion of systematics in the data, and of their comparison to data on simpler conjugated systems for which vibrational band assignments have been made based on the solution of the vibrational eigen value problem, qualitative classification of Raman bands in terms of corresponding atomic motions will be made. Finally, the potential of this technique as a tool for structural studies will be illustrated by some examples involving ligand bending, and reduction-oxidation reactions.

F-PM-3S CONFORMATIONS AND INTERACTIONS OF NUCLEIC ACIDS FROM LASER RAMAN SPECTROSCOPY. Warner L. Peticolas, Department of Chemistry, University of Oregon, Eugene, Oregon 97403

The Raman bands of nucleic acids can be divided into those Raman bands coming from the vibrations of the back-bone supar-phosphate chains and those vibrations coming from the nucleic acid bases. From the frequency of the vibrations of the back-bone chain, one can determine the conformation of the nucleic acid as belonging to the A-family, the B-family or a disordered or partially ordered structure. Studies on the effect of temperature, orientation, fraction water content and solvent composition on a large number of nucleic acid samples allows us to give a mechanism for premelting phenomena in DNA and, also, to show how tertiary structure affects secondary structure. Raman spectra have recently been taken of chromatin samples and it is found from comparison with model compounds that the histones in chromatin are predominately α-helical, that the DNA is of the B-family of conformations and that the N-7 position of guanine represents a very likely site of attachment for the arginine side-chains in chromatin.

F-PM-4S A DESCRIPTION OF RESONANT RAMAN PHENOMENA IN COMPLEX MOLECULES. R. M. Hochstrasser, Department of Chemistry, University of Pennsylvania, Philadelphia, Pa. 19174.

Implications of our recent more complete theory of Raman scattering will be presented in relation to practical questions involved in the interpretation of Raman (off-resonance, near resonance and resonance) spectra of complex molecules. Apart from the usually studied features of band position, polarization and intensity, the additional properties of polarization dispersion, linewidth, and the effect of non-radiative relaxation will be discussed.

As a result of advances in laser technology Raman spectroscopy has become a much more useful structural and analytic tool. The theory of resonance scattering of light leads to results that are already very familiar in the field of single level fluorescence spectroscopy. The differences between conventional fluorescence and coherent Raman scattering will be brought out, again in relation to the resonance spectra of complex molecules including aromatic hydrocarbons and hemeproteins.

F-PM-A1 NON-UNIFORM CONTRACTION OF ISOLATED PAPILLARY MUSCLE. L.L. Huntsman and S.R. Day,* Center for Bioengineering, University of Washington, Seattle, WA. 98195

Microspheres (15μ) infused into the microcirculation were used as markers to define segments within isolated cat papillary muscles. Work by others has shown that the distance between such microspheres is proportional to the average sarcomere lengths in the region between the markers. Video recording and analysis were used to determine the variations of segment lengths as the muscles were allowed to contract isometrically at muscle lengths of 80-100% L_{max}. In all muscles, segments in the center region were found to shorten during muscle isometric contraction while those in the end regions lengthened. Central shortening was typically 5-10% and end lengthening 8-15%. Changes of segment length during contraction were maximum when muscle length was approximately 96% L_{max}. In the passive state, segment lengths varied directly with muscle length over a broad range characterized by low force. Segments in the center region, however, displayed an abrupt transition to high stiffness at a certain length while end regions continued to stretch. Force-length relationships obtained for the presumably healthy center segments are significantly different from those obtained for the whole muscle. The stretch at the ends appears to result from conformational changes and damage caused by the clamping process. Such regions do not appear to behave like simple springs. These results suggest that there may be major difficulties with the interpretation of mechanical measurements on papillary muscles unless stretch of the ends is eliminated or taken into account.

F-PM-A2 POWER OUTPUT AND STIFFNESS CHANGES AT VARIOUS FREQUENCIES OF FORCED SINUSOIDAL OSCILLATIONS DURING SUSTAINED CONTRACTURES IN LIVING CARDIAC MUSCLES. G.J. Steiger*, A.J. Brady and S.T. Tan,* Cardiovascular Res. Lab. UCLA, Los Angeles, California 90024

When sinusoidal length changes are applied the cardiac preparation shows a very distinct and characteristic frequency response in tension and stiffness. 1) There is a well defined narrow frequency range in which the muscle is able to perform work despite a steady state activation. For rabbit papillary muscle at room temperature, f.i., this frequency range is 0.2-0.7 Hz. At low frequencies force and length change are in phase. With increasing frequency a phase lag between length and tension begins to appear giving rise to work output. At the frequency of maximal work output the phase shift may be more than 50° which consequently leads to the paradox phenomenon that the force in muscle still decreases for a period of time despite the fact that it is being stretched. At higher frequencies both work and phase shift diminish until they become zero again. At still higher frequencies the tension change leads the length change indicating that the muscle now absorbs work. 2) In the same frequency range the muscle produces work the dynamic stiffness may drop by as much as a factor of 3: In rabbit, starting with a relatively high stiffness at low frequencies, $\sim$ 60 g/cm^2 x 1% δl, the stiffness drops to a value of $\sim$ 20 g/cm^2 x 1% δl at the frequency at which the phase lag is zero again. At higher frequencies where the muscle absorbs work the stiffness increases steeply. Under investigation have been frog (rana pipiens), bull frog, cat, rat and rabbit cardiac preparations. The time constant of the delayed tension onset and the frequency range of power output are specific for each animal and seem always to be related to the natural heart beat frequency. (Supported by Grant #11351-09 USPHS.

F-PM-A3 RELATION OF FATIGUE STATE IN FROG SINGLE MUSCLE FIBERS TO CONCENTRATIONS OF GLYCOGEN, PHOSPHOCREATINE (PCr) AND ATP. V. Nassar-Gentina*, J.V. Passonneau*, J.L. Vergara*, and S.I. Rapoport, Laboratory of Neurophysiology, NIMH, and Laboratory of Neuropathology, NINCDS, Bethesda, MD 20014

Single muscle fibers of the frog semitendinosus were stimulated in oxygenated Ringer solution at 15° C, at a frequency of 20 Hz for up to 150 sec. After approximately 20 sec of stimulation, tetanic tension began to decline; after 150 sec its mean value was 15% of the initial tension. The fall in tension, characterizing fatigue, was related to fiber metabolism by measuring concentrations of ATP, glycogen, and PCr per mg protein in unstimulated single fibers, fibers stimulated for 30, 100, and 150 sec, and in whole semitendinosus muscles. The fibers were placed in liquid N_2 within 5 sec after termination of the stimulus train. The concentrations of these metabolites did not differ significantly ($P > 0.05$) in unstimulated single fibers and whole muscles. Stimulation of single fibers caused an exponential decline in [PCr] with stimulus duration, with a time constant of approximately 45 sec. After 150 sec, [PCr] was approximately 15% of control concentration, but the concentrations of ATP and glycogen were not different from controls. Although ATP is the immediate energy source for contraction, its rapid resynthesis from PCr probably prevented a measurable decline in its concentration. The results show that muscle fatigue occurred without glycogen depletion, and that PCr was depleted faster than it could be restored by glycolysis and/or oxidative phosphorylation in single fibers.

F-PM-A4 ORIENTATION AND LENGTH OF CROSS-BRIDGES IN CARDIAC AND SKELETAL MUSCLE. T. Iwazumi,* M.R. Byers,* and G. H. Pollack, Depts. of Anesthesiology and Bioengineering, University of Washington, Seattle, WA 98195

The cross-bridge configuration is still an open question. Many models have been proposed (e.g., Huxley & Brown, 1967, and Squire, 1974), but some previously published electron micrographs have shown configurations of bridges unaccounted for by the models. For example, the longitudinal section EM by Carlsen et al. (1961) showed numerous bridges perpendicular to and spanning gap between the thick filaments in the H-zone, and the cross-section EM by Hoyle et al. (1973) showed clearly the existence of lines between thick filaments even in the overlap region.

The orientation and the length of the bridges of moderately stretched skeletal muscle (frog semitendinosus) and cardiac muscle (rat papillary, R.V.) were examined by EM. Results showed that in the overlap region many bridges were seen between thick and thin filaments as well as ones clearly between thick and thick filaments. However, in the H-zone of these muscles, both longitudinal and cross-sections showed numerous long bridges spanning the gap between thick filaments. The orientation and length of bridges observed in the H-zone have not been explained by any models except by one from a field theory (Iwazumi, 1970) which predicted that the projections of the thick filament are: (1) directed toward the adjacent thick filament; (2) helically distributed with 60° rotation per advance in the longitudinal direction; and (3) about 30 nm long. Appearance in EM's of both thick-thick and thick-thin bridges is also explained by the theory.

This research was supported by HL 18676, HL 13517, GM-15591, AHA 63-2517 and 75-WA-516. "Dr. Pollack is an established Investigator of the Am. Ht. Assoc."

F-PM-A5 MAXIMUM VELOCITY AND ISOMETRIC TENSION RELATIVE TO SARCOMERE LENGTH IN INTACT CARDIAC MUSCLE. J.W. Krueger and G.H. Pollack, Anesthesia Research Center, University of Washington School of Medicine, Seattle, Wa. 98195

Velocity of sarcomere shortening at zero muscle tension and isometric tension at zero sarcomere shortening velocity were studied in isolated rat papillary muscles (26° C, field stimulated at 24/min). Sarcomere length was measured by light diffraction. Muscle length was servo controlled: By adjusting the command signal it was possible either to keep sarcomere length constant or muscle tension zero by respectively stretching or shortening the muscle during contraction. Both isometric tension and velocity of unloaded sarcomere shortening reached their peak values relatively early in the contractile cycle. Peak isometric tension increased linearly with sarcomere length from zero at 1.6 μm to a value of 1.2 kg/cm^2 at 2.1 μm. Between 2.1 and 2.3 μm tension appeared to be constant. The velocity of sarcomere shortening in the unloaded contractions was related to length in a fashion similar to that of isometric tension. Peak velocity of sarcomere shortening was 10 μm/sec at 2.1 μm, decreasing to zero at 1.6 μm; sarcomeres never shortened beyond 1.6 μm. One possible explanation for the results is that factors which limit sarcomere shortening velocity also limit muscle tension. (Supported in part by HL 13517, GM 15991, and 1-F-22-HL00170.)

F-PM-A6 LENGTH-TENSION RELATION FOR A SINGLE CELL LAYERED HEART. M. Morad, L. Cleemann*, Y. Goldman*, and D. Mayers*, Department of Physiology, University of Pennsylvania School of Medicine, Philadelphia, Pa. 19174.

The single cell layered heart of the "sea potato" exhibits, like the vertebrate hearts, long action potentials, K-induced contractures, and inotropic Ca response. Electron microscopy showed that each cell has a single myofiber located near the luminal surface. The heart was opened into a single sheet, extended over an aperture (2.25 mm x 4 - 6 mm) and fastened around the edges. When the pressure of the closed lower chamber was increased (1 to 2 cm water), the tissue bulged upward and formed a semi-circular cylindrical surface, resembling a segment of the original tubular structure. A light beam passing through the upper chamber was used to measure the height of the "bulge". Evans Blue dye was perfused in the lower chamber to increase the light blocking capabilities of the bulge and to check for leaks. Servo-control of the bulge height was obtained by feeding back the changes in the light signal to the lower chamber through a motor causing volume displacement. The bulge height was used to estimate the length of the heart. Using Laplace's Law, the tension was calculated from the pressure measured in the lower chamber. With the bulge clamped, increasing the initial length increases the twitch tension linearly to a maximum. Tension then plateaus for a short length and finally falls to zero linearly. The resting tension rises steeply in the region where the twitch tension falls resulting in increasing total tension. The length-tension relation is similar to that obtained from single fibers of sartorius muscle. However, the region where active tension is observed (0.8 l_{max} to 1.15 l_{max}) is only a small fraction of the region in the vertebrate skeletal muscle (0.6 l_{max} to 1.7 l_{max}). Supported by USPHS HL 16152.

F-PM-A7 MEMBRANE CURRENTS IN EMBRYONIC HEART CELL AGGREGATES. R.D. Nathan and R.L. DeHaan, Department of Anatomy, Emory University, Atlanta, GA. 30322.

A microelectrode voltage clamp analysis has been performed on spheroidal aggregates of 7-day embryonic chick heart cells at 36°C. All aggregates used were 140-150μ in diameter. Three-electrode impalements, including a second potential-sensing microelectrode, were used to monitor the spatial homogeneity of the command potential throughout the aggregate volume. Maximal inhomogeneity occurring during the fast inward current was usually less than 3 mV, and less than 1 mV during the remainder of the clamp step. Loss of uniformity as monitored with the third electrode, coincided with increased leakage current, lengthening of the capacitive transient, and prolongation of fast inward current inactivation. The voltage-dependent, fast inward current, which could be blocked by TTX, exhibited a peak amplitude between -40 and -30 mV. Under best conditions, the onset of this inward current could be partially separated from the preceding capacitive transient (whose duration was less than 1 msec) and the current was completely inactivated in less than 1 msec. A slow inward current, blocked by D600, was maximal between -10 and 0 mV. At -10 mV, this inward current was inactivated with a time constant of 6-9 msec. Outward current, not blocked by either TTX or D600, was measured at the end of a 400 msec voltage step. Its magnitude at -30 mV was about 15% of the maximum fast inward current. (Supported by NIH fellowship HL 01321 and grant HL 17827.)

F-PM-A8 EFFECT OF EXTRACELLULAR POTASSIUM ON THE INTRACELLULAR POTASSIUM ACTIVITY OF CANINE CARDIAC PURKINJE FIBERS. D.S. Miura*, M.R. Rosen*, and B.F. Hoffman, Dept. of Pharmacology, College of Physicians & Surgeons, New York, N.Y. 10032.

Potassium (K^+) is the major intracellular cation and the principal determinant of the cardiac Purkinje fiber (PF) resting membrane potential (RMP). To gain greater understanding of the role of K^+ in the electrophysiology of the specialized conducting system of the mammalian heart, we developed a method using open tip microelectrodes containing a K^+ sensitive resin (Corning 477317) to determine directly the intracellular K^+ activity, a_K^i. We measured the effect of changing extracellular K^+ (c_K^o) on transmembrane resting and action potentials (AP), a_K^i, and the K^+ equilibrium potential (E_K) for beating and quiescent PF. During superfusion with Tyrode's solution (c_K^o = 4 mM), control PF transmembrane potentials were measured through 3 M KCl filled microelectrodes. The maximum diastolic potential (MDP) was measured at the point of maximum AP repolarization, and the RMP was measured in quiescent PF 20 sec. after discontinuation of the stimulus. The a_K^i in PF superfused with Tyrode's (c_K^o = 4 mM) was 130.0±2.3 mM (M±S.E.) at 37° C, and the E_K was -100.6±0.5 mV; this is the same as the $i_{K,2}$ reversal potential measured by investigators using voltage clamp. The a_K^i appeared to be independent of c_K^o superfusing the PF when the latter was increased to 6, 10, and 16 mM. Further, RMP varied as a linear function of the logarithm of a_K^o during superfusion with Tyrode's solution in which c_K^o was greater than 6 mM. When c_K^o was 2 mM, a_K^i did not change, and RMP did not increase as predicted for a membrane acting as a K^+ electrode. Hence, the measured a_K^i for c_K^o = 2 to 16 mM was constant, and E_K agreed with voltage clamp data.

F-PM-A9 AN NA-CA EXCHANGE MECHANISM FOR NA-DEPENDENT EXTRUSION OF CALCIUM FROM EXCITABLE CELLS. P.M. Sidell*and J.B. Bassingthwaighte, Department of Surgery, Mayo Clinic, Rochester, Minn. 55901; Center for Bioengineering, University of Washington, Seattle, Wash. 98195.

Kinetic equations for a carrier mediated Na-Ca exchange are used to examine the ability of the Na-Ca exchange hypothesis to describe the Na dependent calcium efflux in excitable tissues. This model describes a system in which the carrier affinity for Na and Ca is different on opposite sides of the cell membrane so that the intracellular Ca concentration, Ca_i is driven to fit the ratio: $\frac{Ca_i}{Ca_o} = \frac{Na_i^2}{Na_o^2} \cdot \frac{K_{iCa}\, K''_{oNa}}{K_{oCa}\, K''_{iNa}}$ The influence of passive membrane permeability to calcium is examined, and the carrier system can be seen as a buffering mechanism for the maintenance of $[Ca]_i$. The ability of the carrier system to stabilize $[Ca]_i$ in the presence of increasing passive Ca influx is determined by $[Na]_i$, $[Na]_o$, $[Ca]_o$, and the amount of carrier present. The equations describe data on Ca flux in guinea pig and rat heart with similar sets of parameters, which also differ little from those describing the influence of Na_o on systolic tension in frog heart or on diastolic tension in rat heart. Approximate values for the binding constants are in the range of the physiological concentrations in ECF or sarcoplasm, and were (molar): $K_{iCa} = 10^{-7}$, $K_{oCa} = 10^{-3}$, $K''_{iNa} \doteq K''_{oNa} \doteq 10^{-2}$. Data on Ca-activated Na flux in squid axon required a different parameter set. The analyses are consistent with localization of this sarcolemmal carrier either to regions in apposition with subsarcolemmal cisternae of SR or in unapposed sarcolemma, and a combination of the two sites would not seem necessary.

F-PM-A10 THE PRIMITIVE ATRIO-VENTRICULAR CONDUCTION PATHWAY IN THE EMBRYONIC MAMMALIAN HEART. C.E. Challice, and S. Virágh‡ The University of Calgary, Calgary, Alberta, Canada T2N 1N4, and Department of Pathology, Postgraduate Medical School, H 1389, Budapest, Hungary

This time last year the present authors reported on the appearance of an A-V "ribbon" of cells at 12 days of embryonic life in the mouse heart, but noted that at that time muscular continuity appeared to be maintained elsewhere around the A-V canal, making it difficult to assign any special electrical role to the ribbon (Biophys. J. 15: 256a). However, more recently, using PAS stain, evidence has been found of the presence of a specialized tract (the A-V tract) 3 days earlier, i.e. only one day after the establishment of regular peristaltic contractions in the primitive tubular heart. At this stage the wall of the A-V canal consists of a double layer of cells, with the tract present in the dorsal inner layer. In addition, recently published work by Pexieder (Adv. in Anat. Embryol. and Cell Biol. 51 #3) has shown that systematic cell death is an important factor in the general embryonic development of the heart, and in the present study, ultrastructural evidence similar to that which he found has been detected in the outer dorsal wall of the A-V canal and (to a lesser extent) in the ventral wall. This suggests that systematic cell death may be the mechanism which creates electrical discontinuity around the A-V canal except for the A-V tract which then becomes the sole electrical link between atrium and ventricle. Later, at 12 days p.c. the primitive A-V node is seen beginning to develop into the A-V cushion from the A-V tract but approximately midway along it. This structure ultimately links up with the developing IA septum, at which time it becomes essentially the definitive A-V node. Attempts have been made to correlate these structural developments with the contractile sequence using cine-photomicrography of the pulsating heart.

F-PM-A11 CHARACTERIZATION OF PHYSIOLOGICAL DIFFERENCES ACROSS CARDIAC TISSUES USING A COMPUTER BASED HEARTMONITOR. D.N. Jones* and M.W. Luttges, Aerospace Engineering Sciences Department, University of Colorado, Boulder, Colo. 80302

Contractile cardiac tissues are exquisitely sensitive to cardioactive drugs but are concomitantly insensitive to normal physiological variations such as changes in heart rate. The observed dissociation between factors which regulate depolarization events at specific anatomical sites and similar factors which control the systematic events of complete cardiac cycles is poorly understood. By employing several cardioactive agents both separately and jointly, the nature of physiological differences across and within the functional subunits of the cardiac system are elucidated. A recently developed computer based heartmonitor provides the resolution necessary to detect the elusive differences between these subunits, e.g., between pacemaker and normal contractile tissue. The monitor employs temporal spread criteria and correlation waveform change on each of the major portions of the EKG. Toxicity studies show that the monitor detects waveform changes of less than 3%. The temporal and correlative resolution is crucial for the dissection of the cardiac system into its physiologically distinct entities.

F-PM-A12 TRANSMEMBRANE POTENTIALS IN SMOOTH MUSCLE OF THE RABBIT MESOTUBARIUM SUPERIUS USING THE SUCROSE-GAP TECHNIQUE. S. A. Halbert, Department of Biological Structure, University of Washington, Seattle, WA 98195

The mesotubarium superius (MTS) of the rabbit is a muscular accessory membrane of the female reproductive tract which exhibits hormonally controlled, spontaneous contractile activity. Transmembrane potentials of the MTS smooth muscle were recorded in vitro, indirectly with extracellular electrodes by using the sucrose-gap technique. A simple electrical equivalent circuit of the sucrose-gap preparation was used to calculate corrections for the effects of liquid junction potentials and short circuiting of the gap. As in other smooth muscles, resting potentials were about 20 mV greater (more negative) when K_2SO_4 was used instead of KCl for a reference depolarization. Direct contribution of liquid junction potentials to the sucrose-gap potentials only accounts for about 20% of the discrepancy between KCl and K_2SO_4 resting potentials. Independent measurements with microelectrodes gave a resting potential halfway between the KCl and K_2SO_4 sucrose-gap values (48 mV for MTS from rabbits at ovulation). Action potential peak amplitudes were variable and ranged from 3-30 mV. The largest variety averaged about 20 mV and all action potentials combined averaged about 15 mV. Calculated values were about 20% greater and were comparable with microelectrode measurements suggesting that short circuiting of the gap was much less detrimental than in most smooth muscle sucrose-gap preparations. MTS from rabbits at ovulation had lower resting potentials (about 10 mV), reduced action potential frequency and approximately equal action potential amplitude compared to rabbits in estrus. This does not account for the observed increase in spontaneous contractile activity of MTS at ovulation. (Supported by USPHS Grant No. 5T1GM00260-13 and NIH Contract No. HD-03752.)

F-PM-A13 TENSION RESPONSES OF DETERGENT TREATED SMOOTH MUSCLE. A.R. Gordon and L.R. Jones*
Physiology Department, University of South Alabama College of Medicine, Mobile, Al. 36688

Initial observations of the tension responses of detergent treated rabbit taenia coli suggest that tension regulation is similar to that of an actin-linked regulatory system. That is, the relationship between tension and [MgATP] seems to be bellshaped with an optimum at about one mM MgATP. However, this conclusion is somewhat clouded by the relatively low and variable tension production (10-30%) by the detergent treated muscle compared to tetanus tension developed by the normal muscle. In order to clarify the effects of the detergent treatment, the duration of the detergent treatment and composition of the detergent solution were systematically varied and the subsequent tension responsiveness to Mg++, ATP and Ca++ were studied. After control tetanus or K-contractures were obtained from the normal muscle in Krebs solution, the muscle was exposed to the experimental detergent solution. Tension responses were then elicited from the muscle by adding solutions containing the following (mM): 5 EGTA+CaEGTA (pCa 7.5-5.0), 10 Mg-acetate, 20 MOPS or Imidazole (pH 7.0), 0.01-10.0 MgATP, and KCl to maintain ionic strength at 0.1 M. Maximum tension of the detergent treated muscle always occurred at 0.5-1.0 MgATP and pCa 5.0. The detergent solutions generally contained 1% Brij-58, 150 mM KCl, 20 mM MOPS or Imidazole (pH 7.0) and 5 mM EDTA or EGTA. Muscles which were exposed to this solution at pCa 7.5, for 15 hours (overnight), developed 39% of control tension. Raising the pCa, reducing the duration of the Brij treatment to two hours, or raising the [Mg++] above contamination levels, reduced the maximum tension the muscle could develop. Except for muscles which were unresponsive (after two hours Brij and high [Mg++]), the relationship between tension and [MgATP] was essentially unchanged by the different treatments. This study was supported, in part, by NIH grant 1 R01 AM18415-01 and an intramural grant from the College of Medicine.

F-PM-A14 FACTORS AFFECTING THE MECHANICAL PROPERTIES OF VASCULAR SMOOTH MUSCLE. J.E. Hartt, B. Gaylinn*, and W.H. Johnson, Dept. of Biology, Rensselaer Polytechnic Inst., Troy, N. Y. 12181

The stiffness of the glycerinated hog carotid preparation has been examined under a variety of conditions. The fiber's stretch resistance in buffer at pH 7.5 was relatively low. Reducing the pH to 6.0 did not alter the stiffness appreciably. If the muscle is then activated to contract with Ca^{++}-ATP, the stiffness increases greatly. Upon removal of the calcium and reduction of the pH to 6.0, the stretch resistance increases further. Raising the pH again to 7.5 causes a reduction of the elastic modulus to the initial low values.

Ionic strength also affects the stiffness of the preparation. The pH-dependent stretch resistance is found to increase with increasing ionic strength from 0.1 to 0.2. Above 0.3, however, the effect is variable, with generally lower stiffness values evident.

Extraction of the fiber bundle with Hasselbach-Schneider media gave the following results: the low pH (6.2) extraction, which is shown by gel electrophoresis to differentially remove actin and myosin, still yielded pH-dependence, although at lower values of stiffness since no contraction could be elicited. The high pH (7.8) extraction, which also removes tropomyosin, showed neither pH-dependence nor contractile activity. It is thus suggested that the tropomyosin-containing large filaments may interact in a fashion similar to that proposed for molluscan smooth muscle via independent linkages.
(Supported by Northeastern N. Y. Heart Assoc.)

F-PM-B1 COMPUTER SIMULATION OF TRANSMITTER RELEASE AT THE PRESYNAPTIC MEMBRANE.
D.E. Downie, Curriculum in Biomedical Engineering & Mathematics, Dept. of Surgery UNC School of Medicine, University of North Carolina, Chapel Hill, North Carolina 27514

A previous model of transmitter release (Downie, J. Theoret. Biol. 28 297 (1970)) includes the following: (1) combination of extracellular calcium with a negatively charged carrier to form an anionic complex; (2) influx of the complex through the membrane during the course of the action potential; (3) combination of the complex with some activator site in the membrane; (4) release of quantal packets of chemical transmitter. This model is extended through the incorporation of a mosaic of release and activator sites, in accordance with electron microscopic evidence (Akert et.al., Prog. Brain Res. 31 223 (1968)). These studies indicated an organization of the presynaptic membrane in which the activator sites are in trigonal array, the release sites in hexagonal array. In this scheme each release site has direct contact with three activator sites, each activator site with six release sites. The former suggests a hypothesis for the observed cooperativity of calcium in the release process (Hubbard et.al., J. Physiol. 194 75 (1968)). The latter suggests that, under conditions where non-Poisson spontaneous release has been demonstrated (Cohen et.al., J. Physiol. 236 363 (1974)), the underlying mechanism may be a common releasing factor.

The model has been simulated on a digital computer, and can be run in a steady-state mode (probabilistic and equilibrium simulation) or in a transient mode (stochastic and kinetic simulation). The immediate object has been to test the capability of the model to represent calcium cooperativity during spontaneous release (this has been demonstrated by steady-state simulation), as well as the non-Poisson spontaneous release with high concentrations of extracellular calcium. A more general role for the model is to provide a methodology to examine the consequences of various hypotheses regarding spontaneous and stimulated release.

F-PM-B2 STATIONARITY AND INDEPENDENCE OF EVOKED SYNAPTIC QUANTAL EVENTS.
A.I. Lisiecki* and G.P. Moore, Department of Biomedical Engineering, University of Southern California, Los Angeles, CA 90007

Several new statistical techniques have been developed to re-examine the question of whether quantal postsynaptic events occur independently and in accordance with an invariant release function. Experiments were performed on the cutaneous pectoris muscle of the frog at low temperatures under conditiens of low quantum content. A new analysis method allows the time of occurrence of individual quantal potentials to be extracted from evoked end-plate potentials which are composed of multiple and nearly synchronous quantal events. Post-stimulus time histograms of quantal occurrences were analyzed in order to test independence of release of quanta within a single response period and between responses in double-pulse experiments. In a typical experiment, our procedures (1) confirmed earlier reports of independence of quantal events within the release period of a first-pulse response; (2) showed not only that total number of quanta per response follow a Poisson distribution but that the bin-by-bin counts are also Poisson distributed; and (3) showed that quantal events during the second pulse response period are independent of the response to a preceding pulse (for double pulses separated by 100-200 msec). In some experiments, however, non-independence of quantal potentials within the second-pulse response period was detected. Such a result can be explained either in terms of interactions between quantal releases or by non-invariance of a pre-synaptic release function. (Supported by NIH Grants RR 07012 and GM 01724.)

F-PM-B3 ACETYLCHOLINE ACTIVATED PERMEABILITY OF NORMAL AND DENERVATED MUSCLES TO ORGANIC CATIONS.
H.R. Guy*, T. Maeno*, R. Morello*, and M.S. Dekin* (Intr. by C. Izzard), Dept. of Biological Sciences, State University of New York at Albany, Albany, N.Y. 12222

The effects of replacement of Ringer Na^+ by monovalent organic cations on the acetylcholine (ACh) activated depolarization of normal frog sartorius muscles have been measured with the moving electrode technique. The ACh activated channel is apparently very permeable to ammonium and its methyl and hydroxymethyl derivatives, and is moderately permeable to guanidine derivatives and tris(hydroxymethyl)aminomethane (Tris). The permeability of alkylol derivatives of ammonium diminished progressively with increase in molecular size. The results suggest that the channel is slightly less than 7 A in diameter. Differences in the biochemistry and physiological responses between normal end-plate receptors and those which develop following denervation have been reported. The effects of replacement of Na^+ by Tris on the dose-response relationship obtained with denervated muscles were studied to determine whether the channels associated with the newly formed extrajunctional receptors differ from those of the end-plate receptors. The results suggest that the permeability of the extrajunctional channels to Tris is approximately the same as that of the end-plate channels. The effects of other cations on the ACh activated depolarization of denervated muscles is presently being studied. (Supported by USPHS grants NS 07681 and NS 05059-01.)

F-PM-B4 ENDPLATE CURRENT FLUCTUATIONS REVEAL ONLY ONE CHANNEL TYPE AT THE FROG NEUROMUSCULAR JUNCTION. V.E. Dionne and R.L. Ruff*, Department of Physiology and Biophysics, University of Vermont College of Medicine, Burlington, VT 05401 and Department of Physiology and Biophysics, University of Washington School of Medicine, Seattle WA 98195

Acetylcholine induced endplate current fluctuations may be used to distinguish between two alternative models of the postsynaptic channel mechanism which is responsible for the endplate potential. We have measured the mean endplate current and the variance of the endplate current fluctuations induced by iontophoretically applied acetylcholine as a function of membrane potential at the frog neuromuscular junction. Endplate regions of Rana pipiens cutaneous pectoris muscle cells, maintained at 16-17°C, were visualized with Nomarski optics and voltage-clamped with two microelectrodes in Ringer's baths containing 100nM TTX. The mean endplate current and its variance were appreciable at membrane potentials positive and negative of the reversal potential, while both decreased to zero at the reversal potential (approximately 0 mV in this study[1]). These observations cannot be reconciled with a molecular scheme in which acetylcholine opens two separate, independent and specific channels for Na^+ and K^+ at the endplate. The result is accurately described by the model in which both Na^+ and K^+ pass independently through the same channel driven by their electrochemical potentials.

1 Colquhoun, et al. Nature 253, 204-206 (1975)

F-PM-B5 VOLTAGE INDEPENDENT ACETYLCHOLINE RECEPTORS IN THE SKATE ELECTROPLAQUE. R. E. Sheridan, Division of Biology, California Institute of Technology, Pasadena, California 91125

Electroplaques from the skate Raia erinacea were voltage clamped using two microelectrodes. Postsynaptic currents (PSC's) were stimulated with a coaxial electrode adjacent to the innervated surface of the electroplaque. Delayed rectification prevented accurate measurements of the PSC at potentials more positive than -50 mV. The duration of the PSC peak decreased at higher temperatures, probably as a result of increasingly synchronous transmitter release. PSC peaks varied linearly with membrane potential and extrapolated to a reversal potential of +5 ± 10 mV. The PSC's decayed exponentially after the peak. The rate constant of this decay did not depend on the membrane potential over the range -50 mV to -150 mV. The rate constant increased with temperature, from 0.08 $msec.^{-1}$ at 11°C to 0.33 $msec.^{-1}$ at 30°C. Bath-applied carbachol (3-9 μM) produced a steady state conductance increase which did not depend on the membrane potential. The voltage independence of the PSC's in the skate electroplaque indicates a difference between the acetylcholine receptor in skate electroplaque and that of the eel, Electrophorus electricus, which shows significant changes in the kinetics and steady state of the PSC over the same range of membrane potentials. This difference may be related to the function of the PSC in the two animals. In skates, the PSC generates the output current of the organ. In eels, the PSC triggers the output current generated by a sodium spike, a spike which would be shunted by continued conductance through postsynaptic channels.
(Supported by NS-11756, MDAA, and a Grass Foundation Fellowship at MBL, Woods Hole.)

F-PM-B6 ON THE RATE-LIMITING STEP IN ACETYLCHOLINE RECEPTOR ACTIVATION. H. A. Lester and R. E. Sheridan, Biology Division, Caltech, Pasadena, California 91125

With Electrophorus electroplaques exposed to steady acetylcholine and carbachol concentrations, we have measured voltage-jump relaxations of the agonist-induced conductance (g). We have also measured decays of neurally evoked postsynaptic currents (PSC's) (Sheridan and Lester, PNAS 72, 3496, 1975). We present one of several plausible models to describe the kinetic and steady-state findings. The receptor binds two agonist molecules in sequence. For a given agonist, the two binding sites have the same V-dependent equilibrium binding constant. However, the rates at the second site are at least five-fold slower than at the first and, in essence, constitute the limiting steps in channel opening and closing. At the slow site, the forward reaction proceeds with the bimolecular rate constant k_{12}; dissociation proceeds with the V-dependent first-order rate constant $\alpha=\alpha_o \exp(V/V_1)$. The nature of the agonist determines k_{12} (typically 10^7 $M^{-1}sec^{-1}$ at 15°) and α_o (typically 1 $msec^{-1}$) but not V_1 (85 mV at 15°). Curare and desensitization reduce k_{12}. The following predictions are verified: a) With a single agonist present, V-jump relaxations display an exponential time course. b) The relaxation rate constant $k= \alpha+[agonist]k_{12}$. c) In the presence of two agonists, relaxations are the sum of two exponentials. d) Small steady-state g varies as $[agonist]^2\exp(-2V/V_1)$. e) In general, steady-state g varies as $(k-\alpha)^2/k^2$. f) The PSC decay rate gives α for acetylcholine. g) If acetylcholinesterase is blocked, receptors buffer [acetylcholine] in a voltage-dependent fashion so that the PSC decay rate decreases to $\alpha'=\alpha_o'\exp(-V/V_1)$, with no change in V_1.

Supported by NS-11756, Muscular Dystrophy Association, and Sloan Foundation.

F-PM-B7 ACETYLCHOLINE RECEPTOR MEDIATED ION FLUX IN ELECTROPLAX PREPARATION. J.P. Andrews*, G.E. Struve, and G.P. Hess* (Intr. by B.M. Siegel), Biochemistry, Cornell University, Ithaca, N.Y. 14853

The mechanism which regulates nerve impulse transmission involves changes in the permeability of neural membranes to Na^+ and K^+ brought about by the binding of chemical mediators to membrane-bound receptors. A direct relationship between the binding of chemical effectors and this ion flux has not been established. Experiments which probe the relationship will be described. The kinetics of acetylcholine receptor mediated $^{22}Na^+$ flux from electroplax microsacs of E.electricus has been analyzed. Only a small fraction of the observed efflux is affected by chemical activators such as carbamylcholine, decamethonium, and inhibitors such as d-tubocurarine. The apparent cooperativity reported in the literature (Kasai & Changeux (1971) J.Membr.Biol. 6, 1-80) is due to $^{22}Na^+$ efflux from nonexcitable microsacs, the main component of the membrane preparation. Near equilibrium the receptor mediated efflux follows a single exponential decay. The process does not show cooperativity under the experimental conditions. d-Tubocurarine is a non-competitive inhibitor of decamethonium-induced $^{22}Na^+$ flux, suggesting that activators and inhibitors of changes in membrane permeability bind to two different sites. These results are in agreement with our earlier equilibrium and kinetic measurements of the interactions of chemical mediators using the same membrane preparation (Bulger & Hess (1973) BBRC 54, 677; Fu et al. (1974) BBRC 60, 1072; Hess et al. (1975) BBRC 64, 1018).

F-PM-B8 RECONSTITUTION OF A SKELETAL MUSCLE ACETYLCHOLINE RECEPTOR INTO PLANAR PHOSPHOLIPID BILAYERS. R. J. Bradley, W. O. Romine, and G. F. Carl*, Neurosciences Program, The University of Alabama in Birmingham, Birmingham, Ala. 35294, and J. H. Howell*, and G. E. Kemp, New York State Dept. of Health, Roswell Park Memorial Inst., Buffalo, N. Y. 14263.

The nicotinic acetylcholine receptor (AchR) from rabbit skeletal muscle has been isolated by extraction with 1% Triton X-100 and affinity chromatography using α-cobrotoxin as an affinity ligand, a technique in use for isolation of AchR from electric fish. This material has been characterized by α-Bungarotoxin (Butx) binding and molecular weight determination by gel filtration on Sepharose 6B. The preparations were found to bind approximately 0.2 nMoles of ^{125}I-α-Butx per mg. protein. When added to the bathing solution of planar phosphatidyl choline bilayers, this material causes large conductance changes that increase at a linear rate with time and are stimulated by carbamylcholine and inhibited by Butx, curare, and Con A. The amount of conductance increment is proportional to the amount of material added. When small amounts of this material were introduced to the bathing solution, quantal conductance changes were observed. The most frequent channel size was approximately 3.5×10^{-11} mho in 1 M NaCl, with other quantal events whose magnitude appeared to be multiples of this basic event. Studies measuring bi-ionic potentials indicated a Na^+/Cl^- selectivity of 3/1 at pH 7.4. It is hoped that these studies will eventually lead to functional reconstitution of the AchR appropriate to the post-synaptic neuromuscular junction.

Supported by USPHS Grant No. NS-11356.

F-PM-B9 A MODEL FOR THE LOCALIZATION OF ACETYLCHOLINE RECEPTORS AT THE MUSCLE ENDPLATE. C. Edwards, and H.L. Frisch, Depts. of Biology and Chemistry, State Univerisity of New York at Albany, Albany, N.Y. 12222.

In the normally innervated neuromuscular junction of the frog or rat, the area of greatest sensitivity to the transmitter, acetylcholine, is the region of the muscle membrane immediately adjacent to the nerve terminal; however, there is a low, but measurable, sensitivity in the adjacent region. The sensitivity to acetylcholine is presumably due to the presence of specific protein molecules, or receptors, which lie in the muscle membrane. One possible model for the localization of the receptors is to assume that the receptor molecules are synthesized throughout the muscle fiber and are inserted at random into the membrane where they are free to diffuse; in the region of the nerve terminal there is a "sticky zone" so that all of the receptors that contact this zone are stuck there. The receptors in both the membrane and the "sticky zone" have a finite half life. To estimate F, the steady state flux of diffusing particles into the "sticky zone", we assume the muscle to be an infinitely long right circular cylinder and the "sticky zone" to be circular. The solution of the steady state diffusion problem can be related directly to the electrostatic problem of the potential of a circular cylinder between two infinite planes (Knight, Proc. London Math Soc. 39: 272, 1935). With that solution, and using values from the literature for: the diffusion constant of proteins in the membrane (2×10^{-9} cm^2/sec), extrajunctional receptor density (5 receptors/μ^2), end plate radius (17μ), and muscle fiber diameter (38μ), F may be calculated to be 4.3 receptors/sec. If the half life of the receptors is 7.5 days, the steady state number of receptors in the "sticky zone" is about 4×10^6, which is to be compared with measured values of $1.6\text{-}4.7 \times 10^7$ receptors in the end plate. (Supported by grants: USPHS NS 07681, NSF NPS 7404171A01, and ACS PRF 3519C5,6).

F-PM-B10 ISOLATION OF TWO NEUROTOXIC PROTEIN FRACTIONS FROM BLACK WIDOW SPIDER VENOM. R.L. Ornberg*, R.M. Meyer*, and T. Smyth, Jr., Department of Biochemistry and Biophysics, The Pennsylvania State University, University Park, PA 16802

Black widow spider venom from whole venom gland homogenate was fractionated by discontinuous polyacrylamide gel electrophoresis. Venom fractions were extracted from gel sections and assayed for toxicity in cockroaches by: 1) injection into nymphs, 2) application to a ventral nerve cord preparation, and 3) application to a neuromuscular preparation. Of the eleven fractions isolated, two fractions having very different mobilities (R_f = 0.40 and 0.77-0.94) demonstrated consistent neurotoxic activity. The more slowly migrating protein (M.W. 125,000, 8-10S) produced a delayed permanent paralysis following injection; it reversibly blocked nerve impulse conduction in the ventral nerve cord; and it accounted for the major action of venom gland homogenate, inducing a large transient rise in the miniature endplate potential frequency at the neuromuscular synapse. The more rapidly migrating fraction quickly produced a reversible paralysis after injection, reversibly blocked nerve impulse conduction in the ventral nerve cord, but had no effect on the neuromuscular synapse. Additional features of these two neurotoxic fractions will be described.

F-PM-B11 NEUROTROPHIC EFFECTS ON PASSIVE ELECTRICAL PROPERTIES OF CHICK SKELETAL MUSCLE IN VITRO. J. K. Engelhardt*, K. Ishikawa, J. Mori*, and Y. Shimabukuro*, City of Hope Natl. Med. Ctr., Duarte, CA 91010.

Trypsin dissociated skeletal muscle cells from 11-12 day-old White Leghorn chick embryos were cultured in the presence or absence of tissue fragments from the ventral half of spinal cords from 4-7 day-old chick embryos. The passive electrical properties of long (1-2 mm), unbranched muscle fibers in 2-5 week-old cultures were determined according to infinite cable theory, using the square wave analysis technique. These measurements indicated that the passive electrical properties of cultured muscle cells were altered by the presence of nerve tissue. Combined nerve-muscle cultures had a significantly smaller mean transverse membrane resistance ($\bar{R}_m$) than the control muscle cultures. The mean membrane capacitance ($\bar{C}_m$), however, was not significantly different in the two types of cultures; therefore, smaller values of R_m in the combined nerve-muscle cultures must be responsible for the significantly smaller values observed for mean input resistance ($\bar{R}_o$), mean space constant ($\bar{\lambda}$), and mean time constant ($\bar{\tau}_m$) in these same cultures. These differences in the passive electrical properties between the two types of cultures were the same as would be expected on the basis of denervation experiments in vivo.

	$\bar{R}_o$(MΩ)**	$\bar{\lambda}$ (mm)***	$\bar{\tau}_m$(msec)**	$\bar{R}_m$(KΩ cm^2)**	$\bar{C}_m$(μF/cm^2)
Control muscle (n=7)	4.7 ± 3.3	0.88 ± 0.31	13.2 ± 9.5	3.6 ± 2.6	5.1 ± 4.7
Muscle & nerve (n=10)	1.2 ± 0.9	0.58 ± 0.34	4.7 ± 2.2	1.1 ± 1.1	8.3 ± 6.3

** $P < 0.01$; *** $P < 0.05$.

F-PM-B12 INFORMATIONAL PROPERTIES OF GROWING OPTIC AXONS. R.K. Hunt, Jenkins Department of Biophysics, Johns Hopkins University, Baltimore, MD 21218.

Individual optic fibers (OF) in Xenopus synapse at specific loci, mapping topographically across the tectum surface and, by single-unit (SU) type, to different depths. The molecular basis of this selectivity is unknown; but documentation of the map at a resolution of 10 ganglion cell (GC) diameters suggests that the system (7×10^5 GC) features up to 2100 discriminations. By multiple rotation/transplantations of early eye-buds, I perturbed GC differentiation and obtained partially-scrambled maps. In Type 1, OFSU were normally responsive but connected at random viz. surface topography of the tectum, and tectal output SU (intertectal relay) had huge receptive fields (RF). Yet the 3 unit types showed normal depth segregation. In Type II, OFSU mapped as a set of X=a lines on the retina to correct rostrocaudal levels, but were random mediolaterally in the tectum (and DV axis of retina); Type III OFSU mapped as a set of Y=a lines to correct mediolateral levels. Both II & III had normal responses and depth segregation of OFSU, elongated RF of output SU. I conclude each OF carries at least three distinct specifiers of retinotectal connectivity, each of which discriminates a different feature of the target and does so independent of the other two. A Cartesian coding system of 30 (Class X) by 30 (Class Y) by 3 (Class of Unit Type) mediates the 2100 discriminations required for point-to-point map assembly.

F-PM-B13 ALTERED TROCHLEAR MOTONEURON ACTIVITY IN RESPONSE TO SUSTAINED TILT IN BEHAVIOR MUTANT (SPASTIC) AXOLOTLS. C.F. Ide*, (Intr. by Martin G. Larrabee), Jenkins Dept. of Biophysics, Johns Hopkins U, Balto., MD 21218.

The behavior mutant, spastic, in the Mexican axolotl shows Mendelian recessive inheritance, coiling and thrashing in place of swimming, and lack of equilibrium. Anatomical and physiological studies show that auricular Purkinje cells fail to migrate antero-dorsally. Evidence for a reduced Purkinje cell projection to motor areas in the spastic lies in the response of trochlear motoneurons to rotation about the longitudinal axis. Trochlear motoneurons inervate the superior oblique muscles and are excited by optic and vestibular input (in these experiments the optic nerves were sectioned). En passant recordings from wild type trochlear nerve show little activity in the level position. The neurons increase their activity during ipsilateral rotation and while being held at sustained ipsilateral tilt. Rotation from ipsilateral to contralateral silences the motoneurons. Spastic trochlear motoneurons show bursting activity at level. They increase activity to ipsilateral, but fail to reduce their discharge rates on rotation to contralateral. Preliminary data indicate that sectioning the main efferent pathway from cerebellum to IV nucleus (brachium conjunctivum) in wild type animals produces equivalent bursting patterns at contralateral tilt as those seen in spastics.

F-PM-B14 MEASUREMENT OF VERY SHORT FLUORESCENCE LIFETIMES WITH A NEW SINGLE PHOTON COUNTING SYSTEM. P.R. Hartig, K. Sauer, C.C. Lo*, and Branko Leskovar*, Chemical Biodynamics Laboratory and Lawrence Berkeley Laboratory, University of California, Berkeley, Ca. 94720

A novel single photon counting fluorescence lifetime system has been constructed that is capable of accurate lifetime measurements below 100 psec. The system design incorporates unique constant-fraction discriminators that exhibit a time walk of under $\pm$ 60 psec for 2 nsec wide pulses of 35 mV to 8 V amplitude. In addition, the photomultiplier (RCA 8850) is specially selected and the operating conditions adjusted for minimum single photoelectron time spread. Measured lifetimes of 4.94 nsec for de-aerated anthracene in cyclohexane, 640 psec for de-aerated diphenyl butadiene in cyclohexane and 90 psec for erythrosin in 40 mM Tricine-NaOH, 2 mM EDTA pH 8.0 were in agreement with reported values in the literature. Certain parameters essential for accurate short lifetime measurements were identified. The lamp profile FWHM is minimized by the use of clean, sharpened electrode tips and the stability enhanced by continuous flushing with dry air. Lamp drifts are further minimized by time averaging of the excitation profile. The emitting volumes of the excitation and fluorescence samples are equalized to assure the same distribution of illumination on the photocathode. Minimizing the difference between excitation and emission wavelengths reduces the shift in pulse profiles caused by different photoelectron kinetic energies. A small amplitude long lifetime artifact detected in most spectra arises from fluorescence processes in colored glass filters and slight mismatches in scattering volume of the excitation and emission samples. Evidence was obtained that the small amplitude early peak observed in all published spectra arises from photons which pass through the photocathode and directly strike the first dynode. The method has been applied to fluorescence lifetime studies of chlorophyll in chloroplasts, alpha-bungarotoxin, and the chemotactic galactose binding protein.

F-PM-C1 THE TRANSMITTANCE PHOTOMETER, A COMPETITOR TO THE ELECTRON MICROSCOPE?
Paul Latimer, Department of Physics, Auburn University, Auburn, AL 36830

Biological cells (1-5 μm diameter) scatter visible light (λ = 0.5 μm) primarily through interference and diffraction. The transmittance photometer which measures total scattering in suspension can be viewed as a "phase contrast" device. It is presently compared with the scanning electron microscope by considering the use of each for the measurement of subtle changes in cell size (changes of 0.01-0.05 μm), in cell shape, etc. From instrument specifications and light scattering theory, it is found that both methods can resolve such structural changes. Natural particle size heterogeniety will adversely influence both determinations, but especially those with the electron microscope. If it is known in advance what structural feature changes, the photometer is advantageous. Without sample preparation it can remotely, nondestructively, and continuously assay structural changes in real time.

F-PM-C2 DYNAMICS OF FLUORESCENCE MARKER CONCENTRATION AS A PROBE OF MOBILITY. D.E. Koppel*, D. Axelrod*, J. Schlessinger*, E.L. Elson * and W.W. Webb, School of Applied and Engineering Physics, Department of Chemistry, Cornell University, Ithaca, New York 14853

We have developed an effective experimental system for the characterization of molecular and structural mobility. It incorporates a modified fluorescence microscope geometry and a variety of analytical techniques to measure effective diffusion coefficients ranging over more than six orders of magnitude (from $\sim 10^{-12}$cm^2/sec to $>10^{-6}$cm^2/sec). Two principal techniques, Fluorescence Correlation Spectroscopy (FCS),[1] and a fluorescence photobleaching technique are employed.[2] In the photobleaching technique, translational transport dynamics are measured by monitoring the transient decay of a spatial gradient of fluorescence that is photochemically induced in a microscopic volume by a short burst of intense laser radiation. In contrast, FCS uses laser-induced fluorescence to probe the spontaneous concentration fluctuations in microscopic sample volumes. The kinetics are analyzed by computing correlation functions of the measured stochastic fluctuations of fluorescence intensity. The optical system and digital photocount correlator designed around a dedicated minicomputer will be described and discussed. The general power of these techniques will be demonstrated with examples from studies conducted on bulk solutions and model bilayer membranes, and on mammalian cell plasma membranes.

[1]E.L. Elson and W.W. Webb, Ann. Rev. Biophys. Bioeng. 4, 311 (1975); D.E. Koppel, Phys. Rev. A 10, 1938 (1974).
[2]See poster presentation "Mobility Measurements by Analysis of Fluorescence Photobleaching Recovery Kinetics " by D. Axelrod, D.E. Koppel, J. Schlessinger, E.L. Elson and W.W. Webb.

F-PM-C3 QUANTITATION OF SURFACE BOUND ANTIBODIES BY ELECTRON EXCITED X-RAY FLUORESCENT SPECTROMETRY. E.M. Goldin, P.M. Corry, and C.H. Granatek* Dept. of Physics, The University of Texas System Cancer Center, M.D. Anderson Hospital & Tumor Inst., Houston, TX 77025.

A technique has been developed for the quantitation of antibody binding sites on individual whole cells. This method yields information about the numerical distribution of antigens on single cells within a given population. The procedure involves labeling the antibody with ferritin, a globular protein with an iron-rich core. After the reaction of the target cells with purified antibody, the cells are spun onto substrate coated EM grids, and fixed. Analysis is accomplished in a modified transmission electron microscope with a Si(Li) X-ray detector mounted 1" from the sample position. Spectra from the multichannel analyzer are analyzed by an on-line computer. The intensity of the characteristic iron X-ray which is proportional to the amount of ferritin, yields quantitative results for labeled antibody bound to the cell surface. The minimum number of detectable bound antibodies is about 10,000. The procedure is currently being applied to two problems; the first is a highly specific system with 2,4,6 trinitrobenzene sulfonic acid as the hapten. The second, with murine fetal antigens, is an investigation of the role of fetal antigens in tumor recognition and rejection. Some preliminary results indicate 460,000 fetal antigen sites on the surface of murine fetal liver cells and 200,000 bound sites on acute lymphocytic leukemia cells, whereas non-fetal cells (Chinese hamster fibroblast cells in culture) show binding of the order of the limit of detectability.

F-PM-C4 IN SITU IDENTIFICATION OF BIOLOGICAL MOLECULES VIA THE FLUORESCENCE EXCITED BY A SCANNING ELECTRON BEAM. Paul V. C. Hough, Wayne R. McKinney*, and Myron C. Ledbetter*, Biology Department, Brookhaven National Laboratory, Upton, New York 11973.

Proteins, nucleic acids and fluorescein-conjugated antibody are shown to be identifiable in situ via the fluorescence excited by the focussed electron beam of a scanning electron microscope. A molecular species is identified by its characteristic fluorescence spectrum and by a characteristic alteration of the spectrum with time under the electron beam. We have studied electron-excited fluorescence from bulk samples of tryptophan, tyrosine, various proteins, purified DNA from Escherichia coli and bacteriophage T4, and ribosomal RNA, and from intact bovine spermatozoa and hamster nuclei. The theoretical resolution limit--about 20 Å--is determined by the known maximum distance for molecular excitation by fast electrons. Direct extrapolation from our observed resolution of less than 1000 Å in the localization of nucleic acid (using a low-efficiency photon detector) leads to an experimental resolution limit of less than 60 Å. Proteins and fluorescein-coupled antibody will have a resolution limit at room temperature of a few hundred angstroms, determined by the rate of destruction of the fluorescing groups.

We are preparing a photon detector of 100-fold higher efficiency, and are preparing to work at liquid-He temperature. Work supported by U. S. Energy Research and Development Administration.

F-PM-C5 MOBILITY MEASUREMENTS BY ANALYSIS OF FLUORESCENCE PHOTOBLEACHING RECOVERY KINETICS. D.Axelrod*, D.E.Koppel*, J.Schlessinger*, E.L.Elson*, and W.W.Webb, School of Applied and Engineering Physics, and Department of Chemistry, Cornell University, Ithaca, NY 14853

Quantitative characterization of lateral molecular and structural motion on membranes and cell surfaces is enabled by our scheme for analysis of the recovery of fluorescence following local photobleaching.[1] In this procedure, a small spot on a two-dimensional fluorescent surface (e.g. a fluorescently-labeled cell surface) is photolytically bleached by brief exposure to an intense focused laser beam, and the subsequent recovery of the fluorescence (excited by the attenuated beam) is monitored. Recovery occurs by replenishment of intact fluorescent chromophore via lateral transport into the bleached spot. Calculations for diffusion and directed translational motion are displayed for both Gaussian and uniform circular laser beam intensity profiles. It is assumed that the photobleaching follows an irreversible exponential decay of fluorescence under uniform illumination in the absence of diffusive recovery and that the bleaching time is much shorter than the characteristic time for transport recovery of fluorescence in the open volume of the illuminating beam. Experimental precautions necessary to obtain quantitative values for diffusion constants by comparison with the theory are discussed. The theory is compared with prototype photobleaching measurements on lateral diffusion in a thin aqueous layer of rhodamine 6G in order to test procedures and appraise the efficiency of the method. Applications (reported elsewhere) encompass slower diffusion processes than are conveniently measured by fluorescence correlation spectroscopy.

[1]For photobleaching recovery methods see M.-M. Poo and R.A. Cone, Nature 247, 438 (1974); R. Peters et al., BBA 361, 282 (1974); and Y. Yguerabide, private communications.

F-PM-C6 LIPOSOME - CELL INTERACTION: A MEANS OF INTRODUCING A NEW ANTIGENIC DETERMINANT INTO THE SURFACE MEMBRANES OF ANIMAL CELLS. F. J. Martin and R. C. MacDonald, Department of Biological Sciences, Northwestern University, Evanston, Illinois 60201.

Under appropriate conditions lipid molecules exchange between bilayer vesicles and cell membranes. It has been suggested that liposome-cell fusion is the mechanism. However, available evidence does not rule out alternative modes of entry such as molecular diffusion. The present study sought to elucidate the mechanism by which an antigenic lipid, 2,4-dinitrophenylated aminocaproyl-phosphatidylethanolamine (DNP-Cap-PE), is transfered from lipid vesicles to cell membranes. Fresh human erythrocytes, suspended in a low salt medium, were incubated in the presence of liposomes composed of, by weight, 10% DNP-Cap-PE, 5% stearylamine, 20% lysolecithin and 65% lecithin. The following observations indicate that as a result of such treatment erythrocyte membranes become sensitive to antiserum specific for DNP: 1) Treated cells fluoresce when stained indirectly with rabbit anti-DNP serum followed by goat anti-rabbit IgG conjugated to fluorescein. 2) When treated cells are exposed to rabbit anti-DNP serum followed by ferritin-conjugated goat anti-rabbit IgG, ferritin molecules are seen to react directly with the red cell membrane under the electron microscope. 3) Erythrocytes treated with DNP-Cap-PE containing liposomes become susceptable to immune lysis in the presence of anti-DNP serum and active complement. These results indicate that DNP-Cap-PE molecules become intimately associated with the the red cell membrane, probably integrated into the lipid bilayer matrix. Direct electron microscopic observation of the interaction of DNP-containing liposomes with red cells indicates that a substantial proportion of the DNP label enters the erythrocyte membrane by liposome-cell fusion. (This research was supported by NIH Grant AI 11428)

F-PM-C7 DETECTION OF IMMUNOLOGICAL REACTIONS AT LYMPHOCYTE SURFACES. E. E. Uzgiris and J. H. Kaplan*, General Electric Research and Development Center, Schenectady, N.Y. 12301.

We have developed an in vitro test of cell-mediated immunity based on electrokinetic measurements by laser Doppler spectroscopy, a technique which allows a rapid display of cell mobility populations and changes in these populations as a result of cell surface reactions.

We have studied the human tuberculin system as a convenient model of cell-mediated immunity. Lymphocytes, from donors who previously had active tuberculosis were incubated with the tuberculin antigen, purified protein derivative (PPD), and their mobility distributions were recorded. Over 70% of these donors had a new population which did not appear in the control lymphocytes, i.e., those not exposed to PPD. Lymphocytes from individuals with negative skin tests showed no mobility changes after incubation with PPD. These correlations suggest that we are indeed observing the specific binding of the tuberculin antigen to sensitized lymphocytes from tuberculin-positive individuals. (Supported by NCI Contract NO1-CP-3-3231).

F-PM-C8 CHANGES IN CELL-SURFACE PROTEIN EXPOSURE AND ENDOCYTOSIS ACCOMPANYING RESISTANCE TO *RICINUS COMMUNIS* LECTIN IN A MURINE LYMPHOMA VARIANT. J.C. Robbins[1]* and G.L. Nicolson[1,2]* (Intr. by L.D. Peachey), [1]Department of Cancer Biology, The Salk Institute for Biological Studies, San Diego, California 92112, and [2]Department of Developmental and Cell Biology, University of California, Irvine, California 92664.

A variant of the murine lymphoma BW5147 was selected by Dr. R. Hyman for resistance to toxicity of the *Ricinus communis* (castor bean) lectin, RCA_{II}. The variant cell line is approximately 200-times as resistant to RCA_{II} as is the parental line, but has lost only 30-40% of the parental RCA_{II} binding. When whole cells are surface-labeled by lactoperoxidase iodination and the iodinated proteins separated by polyacrylamide gel electrophoresis with sodium dodecyl sulfate, two of the proteins labeled on the parental, sensitive cell line are very lightly labeled (if at all) on the RCA_{II}-resistant variant. The larger of these proteins, about 80,000 daltons, is retained upon RCA_{II}-affinity chromatography of detergent extracts of sensitive cells. The combination of exposure to lactoperoxidase on intact cells and binding to RCA_{II} in extracts implies that this protein is a receptor for RCA_{II} on the cell surface. Its decrease in amount or exposure on the extremely resistant variant cells suggests that it may be a particularly important receptor for cell entry of the RCA_{II}. The smaller selectively-labeled protein, around 35,000 daltons, is not retained by the immobilized lectin. Electron microscopic studies using ferritin-RCA_{II} suggest that the variant cells may be defective in the endocytosis of RCA_{II}.

F-PM-C9 SURFACE CHARGE DENSITY OF RAT CELLS TREATED WITH CONCANAVALIN A. R. P. Milito* and P. Todd, Department of Biochemistry and Biophysics, The Pennsylvania State University, University Park, Pennsylvania 16802

It has been repeatedly reported that concanavalin A (and other plant lectins) selectively agglutinate malignant, transformed, and trypsin-treated cells. Many attempts have been made to establish a relationship between cell surface charge density and cell adhesion. Because lectins selectively agglutinate we wished to determine whether concanavalin A also selectively affected the cell surface charge density as determined on the basis of electrophoretic mobility. A modified Zeiss (Cytopherometer) apparatus was used to measure electrophoretic mobilities of glutaraldehyde-fixed rat erythrocytes, trypsinized whole rat embryo (WRE) cells from monolayer cultures, non-trypsinized WRE cells from suspension cultures, and virus transformed rat XC cells from suspension and monolayer cultures before and after incubation for 0.5-2.0 hr in 1 mg/ml of concanavalin A in phosphate buffered saline or sucrose-glucose solutions. The concanavalin A treatment caused a small (19% and 27%, respectively) but significant decrease in the electrophoretic mobilities of fixed rat erythrocytes in the presence and absence of sucrose and glucose at high ionic strength. Concanavalin A did not reduce the mobility of transformed XC cells or WRE cells under any of the conditions tested. It significantly increased the mobility of trypsin-treated transformed XC cells, but not of WRE cells, in the sucrose-glucose containing buffer at low ionic strength. Trypsin treatment alone decreased the mobility of XC cells by 50% but did not affect the mobility of WRE cells. The effect of concanavalin A on surface charge density, as determined by electrophoretic mobility, is specific for these transformed cells only if they have been treated with trypsin. Supported by Grant No. R01 CA 12589 from the U. S. National Cancer Institute.

F-PM-C10 EVALUATION OF A KINETIC MODEL FOR HEMAGGLUTINATION IN A BINARY CELL SYSTEM. M.J. Lee and B.J. Oberhardt, Technicon Science Center, Tarrytown, N.Y. 10591

Hemagglutination was studied for a binary cell system consisting of antibody coated Rh_o+, and either Rh_o+ or Rh_o- uncoated red cells. The cells were brought into very close proximity by the addition of a cationic polyelectrolyte and then redispersed by addition of anions. After this step, only cells which had formed antibody "bridges" remained aggregated. The fraction of cells free and aggregated was obtained for each component of the binary cell mixture. A kinetic model was constructed for this system based on the physical processes described above. The model included two stages: 1)formation of polyelectrolyte bound preaggregate groupings of cells, and 2)release of either free or aggregated cells from these interim groupings, and trapping of cells devoid of antigen or antibody by clumps of aggregated Rh_o+ cells. This model, in order to fit the experimental data, required that one aggregated cell trap as many as 25 Rh_o- cells - a requirement that was deemed improbable. It was concluded that some additional mechanism must exist for the aggregation of Rh_o- cells. We hypothesize that, when cells are close together in the polyelectrolyte induced state, antigens may transfer from one cell to another. Rh_o- cells could then remain aggregated even in the presence of very few Rh_o+ cells. Comparison of predicted vs. observed data for this model shows excellent correlation.

F-PM-C11 STRUCTURAL REQUIREMENTS FOR COLLAGEN-PLATELET INTERACTIONS. C.L. Wang*, A. Schwartz*, T. Miyata*, A.L. Rubin, and K.H. Stenzel, Rogosin Kidney Center, Departments of Biochemistry and Surgery, Cornell Colleges of Medicine and Engineering, Ithaca and New York City, N.Y.

Collagen interactions with platelets are important for hemostasis in health and may be important in the genesis of some diseases in man. The present study was designed to determine the critical structural requirements for collagen-platelet interactions and, specifically, to determine the effects of side-chain modifications and polymeric structure of collagen on platelet aggregation. Since many chemical modifications of collagen alter its solubility in platelet-rich plasma at physiologic pH, we first prepared native collagen fiber and then stabilized it with either glutaraldehyde or ultraviolet light irradiation. This collagen was then chemically modified by methylation, succinylation, acetylation, and treatment with FDNB or trinitrobenzenesulfonic acid, and maintenance of native fiber structure was confirmed by electron microscopy. Segment-long spacing (SLS) collagen was stabilized with glutaraldehyde, and amorphous collagen fiber was prepared by salt precipitation. Platelet aggregation was quantitated in a platelet aggregometer. None of the maneuvers used to block NH_2 groups eliminated platelet aggregation. Methylation (masking COOH groups) did result in a variable but distinct decrease in platelet aggregation. However, all of the maneuvers that resulted in monomeric collagen at physiologic pH also resulted in loss of platelet aggregation. SLS collagen was similarly inactive in causing platelet aggregation, as was amorphous collagen fiber. These studies indicate that the polymeric structure of collagen is of overriding importance in its ability to cause platelet aggregation, and strongly suggest that a regularly staggered collagen polymer is essential.

F-PM-C12 CELL-MEMBRANE RESPONSES DURING DYNAMIC OSMOTIC HEMOLYSIS. J. P. Yee* and H. C. Mel, Division of Medical Physics and Donner Laboratory, University of California, Berkeley, California 94720

Hemolysis, following exposure of red blood cells (RBC) to unphysiological conditions or agents, is a complex, multi-step process for which various features of membrane structure and function come into play. The escape of intracellular hemoglobin does not necessarily involve permanent loss of integrity of the membrane. The typical "osmotic fragility" test which measures an apparent fraction of cells hemolyzed is a single, "long-time" measure which cannot reveal information on mechanisms preceeding or following lysis. The technique of "resistive pulse spectroscopy" (RPS), recently introduced to better define cell size and to provide a new measure of cell-membrane deformability (Mel and Yee, Blood Cells 1, 391-399, 1975), has now been applied to study the dynamics of early events in RBC osmotic hemolysis. From RPS spectra taken continuously (5 sec. intervals), the time course has been determined for both size and deformability changes resulting from suspension of human RBC populations in media of milliosmolarity 50 to 300. The following distinct, sequential response-phases are discerned: I. swelling to a "critical" volume, approximately twice the normal RBC volume; II."instantaneous" (cell-by-cell) hemolysis, leading to highly deformable ghosts; III."resealing" and loss of deformability of the ghosts. The heterogeneity of the cell population is clearly evidenced in these measurements. Under conditions of more severe osmotic stress, the rate of membrane resealing is seen to be reduced, and the recovery of osmotic responsiveness of the ghosts (or membrane fragments) altered. (Supported by ERDA and NIH, Biophysics Training Grant).

F-PM-C13 THE AGE RELATED DIFFERENCES IN THE KINETICS AND THERMODYNAMICS OF THERMAL INDUCED LYSIS OF THE RED BLOOD CELL. D. A. Juckett, Biophysics Department, Michigan State University, East Lansing, Michigan 48824

The kinetics and thermodynamics for thermal lysis in red blood cells was studied. This cell is used as a model system for unicellular aging without repair mechanisms. Different age populations of a group of RBC's were separated on a Ficoll density gradient. The age stratification was verified by radioactively pulsing the animal (sheep) with Fe^{59} - citrate. This is selectively taken up in newly formed blood cells and provides a marker for a population of cells as they age. Younger and older populations of cells were taken off the gradient and their kinetics of thermally induced lysis examined over the temperature range 42-56°C. The kinetics differ between the populations; they are not exponential in form but are best described by Gompertz and power law kinetics. The data will be presented as computer analysed, best fit curves for both the kinetics and the Arrhenius plots. The latter will be used to determine differences in the activation enthalpy as a function of age. This work was supported by funds from NIH Training Grant #GM-01422 and the College of Osteopathic Medicine of Michigan State University.

F-PM-C14 RELATION OF ULTRASTRUCTURE TO CANCER INVASIVENESS. D.A. Whaley and D.F. Parsons, Electron Optics Laboratory, Roswell Park Memorial Institute, Buffalo, New York 14263

Whether progression between two of the later stages of malignancy, from preinvasive primary (intraductal) to a metastatic secondary tumor cell in the same patient involves recognizable changes in that cell or a change in the extrinsic non-cancer cells along the margin of contact is being studied by stereo high voltage electron microscopy (HVEM) of semithin sections (SS), 0.5-1.0 μ, of human breast carcinoma. Surface topography [1] and cytology, particularly of cytoplasmic microfilaments, are being studied both at the interior of the preinvasive and metastatic tumors and at their contact boundary with non-cancer cells. Breast cancer was chosen to study invasion because it (1) metastasizes through lymphatics, (2) is accessible surgically, (3) is of high incidence, (4) is fatal if untreated, (5) is easily processed soft tissue, (6) is usually excised totally for frozen section diagnosis, (7) often followed by block removal of regional lymph nodes, and (8) corresponds to well-studied animal models. Patients are selected with metastatic infiltrating ductal carcinomas. Concurrent intraductal carcinoma or atypical hyperplasia are found in over 3/4 of these cases [2]. Tissue blocks in Epon are screened first by SS stained for the light microscope by hematoxylin and eosin [3], then by ultrathin sections in an 80 KV electron microscope. Suitable blocks for the HVEM are cut in SS, electron stained, photographed and interpreted in stereo [4]. Questions being studied are (1) does the structure of preinvasive primary tumor differ from that of metastases and (2), at the cancer/non-cancer margin, does the marginal row of cells, on either side, show cytologic degeneration, both for preinvasive primary and for metastases? [1] Spring-Mills and Elias Science 188 (75):947;[2] Gallager and Martin Cancer 23 (69):855; [3] Chang Arch.Path. 93 (72):344; [4] Favard and Carasso J. Microscopy 97 (73):59.

F-PM-D1 THE ISOLATION AND CHARACTERIZATION OF TEMPERATURE-SENSITIVE MUTATIONS OF THE BLUE-GREEN ALGA, SYNECHOCOCCUS CEDRORUM. L. A. Sherman and D. Rice*, Division of Biological Sciences, University of Missouri, Columbia, Mo. 65201.

Temperature-sensitive mutations of Synechococcus cedrorum were isolated after nitrosoquanidine mutagenesis, ampicillin enrichment and replica plating at 26° and 40°C. Many of the mutations are unable to grow at 40°C and have a plating efficiency at least 10^4-fold lower at the higher temperature. Using the selection procedure of Bennoun & Levine (Plant Physiol. 42,1284 (1967)), mutations were isolated which grow at 40°C but are characterized by abnormally high fluorescence. One of these mutations, ts1, was characterized further as to fluorescence kinetics, photosynthetic activity and protein content. The fluorescence of ts1 is 3 to 4-fold higher than that of the control and the induction kinetics in the presence of such compounds as DCMU and DBMIB are substantially changed. Both Photosystem I and II function at the high temperature, but O_2 evolution is inhibited more than 50% at 40°C from the control level. Absorption spectra of the mutant grown at different light intensities at 40°C showed that the chlorophyll to phycocyanin ratio is more sensitive than the control to environmental conditions. The proteins of both ts1 and wild-type were studied by SDS acrylamide gel electrophoresis utilizing 10% and gradient gels. In all cases, the protein composition of ts1 differed in the 15-20,000 dalton molecular weight range. When grown at 40°C, ts1 accumulated a large amount of material banding at about 15,000 daltons, which was not found in the control, while at least one band found in the control was missing. This research was supported by NIH grant GM21827.

F-PM-D2 RECONSTITUTED INTERACTIONS BETWEEN ANTENNA AND REACTION CENTRE COMPONENTS OF THE PHOTOSYNTHETIC MEMBRANE FROM RHODOPSEUDOMONAS SPHAEROIDES
P. Heathcote and R. K. Clayton, Department of Genetics, Development and Physiology, Plant Science Building, Cornell University, Ithaca, NY 14853

Energy transfer between antenna pigment protein and reaction centres from Rps sphaeroides has been successfully reconstituted. The absolute quantum efficiency for bacteriochlorophyll photo-oxidation in reaction centres in the reconstituted system approached unity, when using exciting light wavelengths corresponding to the major absorption peaks of the antenna pigment-protein. Flourescence yields from the isolated antenna pigment-protein and the reconstituted system were comparable with those from purified chromatophores from the nonphotosynthetic mutant PM-8 and from wild-type Rps sphaeroides. Flourescence induction transients typical of the intact membrane were exhibited by the reconstituted system.

Supported by ERDA Contract AT(11-1) 3162 and NSF Grant No. GB. 36591 X.

F-PM-D3 EVIDENCE FOR A UNIT MEMBRANE ASSOCIATED WITH THE BACTERIOCHLOROPHYLL REACTION-CENTER COMPLEX OF GREEN BACTERIA. John M. Olson, Elizabeth K. Shaw*, and Alice L. Comins*, Biology Department, Brookhaven National Laboratory, Upton, New York 11973.

Bacteriochlorophyll reaction-center complexes from Chlorobium limicola f. thiosulfatophilum 6230 (Tassajara) were pelleted, fixed with glutaraldehyde, stained with OsO_4, dehydrated, and embedded in Epon. Thin sections (approx. 60 nm) were stained successively with uranyl acetate and lead citrate and then examined in a Philips EM-200 electron microscope. These sections were populated with distinctive "railroad-track" structures running in all directions. Each structure consisted of two dark "rails" separated by a light space approx. 2 nm wide. Overall width of the "tracks" was 8 ± 2 nm. Lengths varied from 18 to 45 nm, but most were between 25 and 35 nm. These "track" structures indicate the existence of unit membranes in the bacteriochlorophyll reaction-center preparations. When a preparation is treated with 2M guanidine-HCl and chromatographed on Sepharose 4B, bacteriochlorophyll proteins are separated from the reaction-center complex. The remaining complex contains bacteriochlorophyll a, cytochrome 552 and cytochrome 562. Light causes the simultaneous oxidation of cytochrome 552 and reduction of cytochrome 562. Studies of this complex with the electron microscope are in preparation. Research carried out under the auspices of the U. S. Energy Research and Development Administration.

F-PM-D4 SEMIQUINONES IN PHOTOSYNTHETIC SYSTEMS. Brian J. Hales, Department of Chemistry Louisiana State University, Baton Rouge, Louisiana 70803.

Numerous esr signals have been observed in photosynthetic systems which have been assigned to radicals of various quinones and quinone derivatives. Because these radicals are often associated with large protein, membrane or cellular fragments, the spectra observed are powder spectra attributable to immobilized molecules. In order to better understand and identify the environment of these radicals, model systems have been constructed for observation of the immobilized semiquinone in polar and nonpolar as well as aqueous and aprotic solvents. Spectra will be shown of the immobilized semiquinone anion and neutral semiquinone radicals of both ubiquinone and plastoquinone in these various solvent systems. Comparison of these spectra with the previously observed in vivo semiquinones shows the possible presence of two different environments for the ubiquinone anion in photosynthetic bacteria and the tentative identification of signal II observed in green plant and algae systems with neutral plastosemiquinone.

F-PM-D5 TIGHTLY BOUND UBIQUINONE AND PHOTOCHEMICAL ACTIVITY IN Rhodospirillum rubrum, L.E. Morrison*, J.A. Runquist* and P.A. Loach, Department of Biochemistry and Molecular Biology, Northwestern University, Evanston, Illinois 60201.

Although ubiquinone extractions of chromatophores have been conducted previously by others, the methods used generally lacked the sensitivity required to obtain quantitative information with regard to residual quinone content. A sensitive determination of ubiquinone was made possible by growing cells in media containing ^{14}C p-hydroxybenzoic acid which gave a high incorporation of radioactivity into ubiquinone, as previously described by Rudney and Parson. Chromatophores were extracted with a number of hydrocarbon solvents and the ubiquinone isolated on silica gel thin layer plates. Losses of quinone during the procedure were accounted for by use of carrier technique. Ubiquinone in the residue which was not extracted with the hydrocarbon solvents, was extracted with 1:1 acetone-methanol and determined as above. Finally, the amount of radioactive material resisting all extraction was determined. Analysis of all protein components of chromatophores indicated <0.06 mole ubiquinone/trap could be covalently bound to protein. The extraction data showed the existence of two separate ubiquinone pools, one easily extractable in hydrocarbon solvents and one remaining tightly bound to chromatophores. The loosely bound pool consisted of 5.0 ubiquinone per trap. Single-flash absorbance change data and low temperature light-induced ESR signals determined that removal of the loosely bound pool did not diminish the primary photochemistry. When the loosely bound pool was removed from labelled chromatophores and cold ubiquinone added back, little if any exchange occured between the hot and cold ubiquinone pools. The tightly bound pool had a higher specific activity than the loosely bound pool. Quantitative estimation of the moles of tightly bound ubiquinone per mole primary electron donor unit gave 0.48 + .06 (s.d.) in seven separate experiments.

F-PM-D6 THE QUANTUM EFFICIENCY OF BACTERIOCHLOROPHYLL PHOTO-OXIDATION IN PHOTOSYNTHETIC REACTION CENTERS FROM RHODOPSEUDOMONAS SPHAEROIDES AT TEMPERATURES FROM 300K TO 4K. R. K. Clayton and T. Yamamoto, Section of Genetics, Development and Physiology, Cornell University, Ithaca, New York 14853

The quantum efficiency of bacterochlorophyll photo-oxidation in reaction centers from Rps. sphaeroides was determined by measuring the rate of the light-induced absorbance change at 870 - 890 nm. The efficiency was found to be independent of temperature, within confidence limits of 15 per cent, from 300K to 4K. The value at room temperature had previously been shown to be 1.02 ± 0.04 (C. A. Wraight and R. K. Clayton, 1973. Biochim. Biophys. Acta 333, 246-260).

Absorption spectra of reaction centers show that 535 - 540 nm absorption band of bacteriopheophytin is resolved at low temperature into components with maxima at 532 and 544 nm. The spectrum of the light-induced change "p^{f}" (W. W. Parson, R. K. Clayton and R. J. Cogdell, 1975. Biochim. Biophys. Acta 387, 265-278) shows a sharp minimum near 542 nm (M. G. Rockley, M. W. Windsor, R. J. Cogdell and W. W. Parson, 1975. Proc. Natl. Acad. Sci. U. S. 72, 2251-2255). If this change reflects electron transfer from bacteriochlorophyll to bacteriopheophytin, as suggested by J. Fajer (verbal communication), only one of the two molecules of bacteriopheophytin in each reaction center appears to be involved.

Supported by Contract No. AT(11-1)-3162 from the U. S. Energy Research and Development Administration and by Grant GB36591X from the National Science Foundation.

F-PM-D7 THE CAROTENOID ABSORBANCE CHANGE AND ENERGY TRANSDUCTION IN CHROMATOPHORES
M. Baltscheffsky* (intr. by A. Ehrenberg) Dept. of Biochemistry, Arrhenius Laboratory, University of Stockholm, S-104 05 Stockholm, Sweden.

The light induced carotenoid absorbance change in chromatophores from R. rubrum has been studied with varying light intensities. The two different kinetic phases of the change ($t_{1/2}$ < 2 μsec and $t_{1/2}$ = 10 msec) are saturated at different light intensities under continuous illumination. The slower phase is abolished in the presence of the electron transport inhibitors antimycin and dibromothymoquinone, or by the removal of the coupling factor ATPase from the chromatophore membrane. This makes it possible to study the fast phase alone. Saturating intensities for the fast phase and the total change are, respectively, 10^5 and 10^6 ergs/cm^2/sec. In order to elucidate which part(s) of the energization process is reflected by the carotenoid change comparison with light saturation curves for photophosphorylation to ATP and PPi as well as the formation of pH-gradient and membrane or localized potential have been made. The rate of PPi formation is saturated at low light intensities (Guillory and Fischer, Biochem. J. 129 (1972) 471). We find the tight induced response of the potential indicating exogenous probe merocyanin V to be saturated at low intensities. In contrast, the rate of photosynthetic ATP synthesis and the rate of pH change both are saturated at the higher intensities. The relationship between these results and membrane linked phenomena that may give rise to the two different kinetic phases of the carotenoid absorbance change will be evaluated, and the possibility that the slow phase is the result of a conformation change in the coupling factor region will be considered.

F-PM-D8 THE PRIMARY ELECTRON ACCEPTOR IN CHROMATIUM VINOSUM (STRAIN D).† M. Y. Okamura, L. C. Ackerson,* R. A. Isaacson,* W. W. Parson, and G. Feher, Department of Physics, University of California, San Diego, at La Jolla, CA 92093, and Department of Biochemistry, University of Washington, Seattle, WA 98195.

The primary electron acceptor in photosynthetic reaction centers of Rhodopseudomonas spheroides has been proposed to be a ubiquinone-Fe^{2+} (ferroquinone) complex [M.Y.Okamura, R.A.Isaacson, and G. Feher, P.N.A.S. 72, 3491 (1975)]. However, chromatophore preparations from Chromatium vinosum (Strain D), which were extensively extracted with petroleum ether, were reported to contain no ubiquinone while still retaining photochemical activity [W. W. Parson and R.J.Cogdell, Biochim. Biophys. Acta 416, 105 (1975)]. In order to investigate the question of the primary acceptor in Chromatium, we examined such chromatophores for other quinones and found that they retain ∿ 1 molecule of a menaquinone (Vitamin K) per reaction center. In addition, we have prepared Chromatium reaction centers by the method of Lin and Thornber [L.Lin and J.P.Thornber, Photochem. Photobiol. 22, 37 (1975)], which were depleted of excess quinones by treatment with 1% Triton X-100, 10 mM o-phenanthroline, pH 8. These reaction center preparations are photochemically active at cryogenic temperature and contain ∿ 1 menaquinone/reaction center, but < 0.1 ubiquinone/reaction center. Both chromatophores and reaction centers exhibit a broad, g = 1.8, light-induced EPR signal similar to that seen in R. spheroides. We propose that in Chromatium, as in R. spheroides, the primary acceptor is a quinone-Fe^{2+} complex. However, in Chromatium, this quinone is a menaquinone.

†This work was supported by NSF Grants BMS 74-21413 and BMS 74-19857, NIH Grant GM-13191, and by a Career Development Award (to M.Y.O.) #1 K04 GM 00106-01.

F-PM-D9 LOCALIZATION OF REACTION CENTER PROTEIN IN CHROMATOPHORES FROM RHODOPSEUDOMONAS SPHEROIDES BY FERRITIN LABELING.† G. Valkirs,* D. Rosen,* K. T. Tokuyasu,* and G. Feher, U.C.S.D., La Jolla, CA 92093.

Reaction centers (RCs), isolated from R. spheroides R-26, are composed of three subunits, L(21 Kd), M(24 Kd), and H(28 Kd) [Okamura, et al., Biochem.(1974) 13, 1394]. Immunization of rabbits with RCs and with the purified H subunit yielded antisera against these immunogens. Chromatophores were separately incubated with anti-RC IgG, anti-H IgG, and normal IgG, washed, and then incubated with goat anti-rabbit IgG-ferritin conjugate. Chromatophores were separated from unreacted ferritin conjugate by sucrose gradient centrifugation, fixed, and embedded for electron microscopy. The electron micrographs revealed extensive ferritin labeling of the outside of the chromatophore membrane in both anti-RC IgG and anti-H IgG treated chromatophores (see Fig.), but no labeling of chromatophores treated with normal IgG. This indicates that RCs and the H subunit are both exposed at least on the outside surface of the chromatophore membrane which is in agreement with previous findings [Steiner, et al., Fed. Proc. (1974) 33, Abstract #1345, and Reed, et al., B.B.A. (1975) 387, 368]. Currently, antibodies against the LM unit are being produced and sodium cholate is being used as a means to expose the inside of chromatophores to antibodies. Ferritin labeling of both spheroplasts and frozen sections of whole bacteria is also in progress. Goat anti-rabbit IgG and ferritin were the generous gifts of Dr. S. J. Singer.

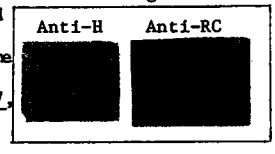

†Work supported by NSF Grant BMS 74-21413 and NIH Grants GM-13191 and GM-15971.

F-PM-D10 IRON-SULFUR PROTEINS OF THE GREEN PHOTOSYNTHETIC BACTERIUM *Chlorobium*.
D. B. Knaff and R. Malkin, Department of Cell Physiology, University of California, Berkeley, California 94720.

The iron-sulfur proteins of the photosynthetic green sulfur bacterium *Chlorobium* have been characterized by oxidation-reduction potentiometry in conjunction with low-temperature electron paramagnetic resonance spectroscopy. Four chromatophore-bound iron-sulfur proteins were detected. One is the "Rieske" type iron-sulfur protein with g-values of 1.90 and 1.79 in the reduced state. The *Chlorobium* g = 1.90 protein has a midpoint potential of +160 mV (at pH 7.0), and this potential is pH-dependent. The oxidation-reduction properties of this protein are markedly different from those of the g = 1.90 proteins in other photosynthetic organisms, where the midpoint potentials are near +290 mV and pH-independent. The potential of the *Chlorobium* g = 1.90 protein correlates with the observation that other *Chlorobium* electron carriers, such as cytochrome *c* and reaction-center bacteriochlorophyll, have less positive potentials than do comparable carriers in other photosynthetic organisms. Three g = 1.94 chromatophore-bound iron-sulfur proteins were observed, with midpoint potentials of -25 mV, -175 mV, and approximately -550 mV. The -550 mV iron-sulfur protein may function as the primary electron acceptor in *Chlorobium*. A low-potential primary acceptor is expected because *Chlorobium* chromatophores are capable of a direct ferredoxin-dependent uncoupler-insensitive photoreduction of NAD and of photochemical reactions at potentials more negative than -450 mV. Chromatophores from *Chromatium vinosum* and *Rhodospirillum rubrum*, bacteria that cannot directly generate reductants more negative than -180 mV, contain none of this low-potential iron-sulfur protein.

Supported in part by NSF grants BMS-75-19736 and BMS-75-18879.

F-PM-D11 A NEW METHOD FOR DETERMINING THE SIGN OF THE ZERO FIELD SPLITTING PARAMETERS IN EXCITED TRIPLET STATES. APPLICATION TO PHOTOSYNTHETIC BACTERIA.
J. R. Norris* and M. C. Thurnauer* (Intr. by Robert E. Krisch), Chemistry Division, Argonne National Laboratory, Argonne, Illinois, 60439

In our studies of the magnetic properties of the lowest triplet state of the chlorophylls it is necessary to determine the sign of the zero field splitting parameters. This enables one to better understand the changes in these parameters in the various chlorophylls studied *in vitro* and *in vivo*. The electron spin polarization in these systems precludes the possibility of using the standard methods for the sign determination. We have developed a method for determining the sign of D based on the spin lattice relaxation properties of these systems. Our results show that $D > 0$ in the triplet observed *in vivo* in photosynthetic bacteria. This further substantiates our proposed mechanism for the primary photoact in bacterial photosynthesis (1). This information together with recent magnetophotoselection experiments on these systems has led to further understanding of the chlorophylls.

(1) M. C. Thurnauer, J. J. Katz and J. R. Norris, Proc. Nat. Acad. Sci., U.S.A., 72, 3270 (1975).

F-PM-E1 EQUATIONS FOR MEASURING THE RATE OF DNA CHAIN GROWTH AND REPLICON SIZE BY DENSITY LABELLING TECHNIQUES. Joseph L. Roti Roti and Robert B. Painter, Department of Radiology, University of Utah 84132 and The Laboratory of Radiobiology, University of California, San Francisco, California 99143.

The effects of initiation, termination and clustering of replicons have been considered in the development of equations which are used to measure DNA chain elongation in mammalian cells by density gradient techniques. These equations can be used to determine the average replicon size as well as the rate of chain elongation. Experimental data from WI-38 and HeLa cells are presented which show the applicability of these methods. Eight different models of replication initiation and termination have been developed. Some of these models can be eliminated experimentally and the experimental results are consistent with the notion that neighboring replicons are initiated simultaneously or sequentially with short (≃ 0.5 min.) interinitiation time.

F-PM-E2 CONTROL OF DNA HELIX OPENINGS DURING GENE REGULATION. J.H.Frenster, S. Landrum*, M.A.Masek*, and S.L.Nakatsu*. Department of Medicine, Stanford University, Stanford, Calif.

Both carcinogenic chemicals (Nature 257, 151 (1975) and oncogenic viruses (Virology 65, 524 (1975) prefer to bind to single-stranded portions of the host genome (Biophysical J. 15, 137a (1975). Localized DNA helix openings are necessary to allow the initiation of either selective gene transcription or asynchronous gene replication (Nature 208, 894 (1965). We have developed a high-resolution electron microscopic technique for directly analyzing DNA helix openings within living cells (Nature New Biol. 236, 175 (1972), and have quantitated this technique for use within individual cells undergoing cell division and cell differentiation in human bone marrow (Nature 248, 334 (1974). 123 normal differentiating granulocyte precursor cells, 189 normal differentiating erythrocyte precursor cells, 97 normal marrow mononuclear cells, and 22 normal differentiating megakaryocyte precursor cells were analyzed as were 55 normal mitotic bone marrow cells. DNA helix openings were found only within the euchromatin portion of the cell nucleus. During normal bone marrow cell differentiation and during the prophase, metaphase, anaphase, and early telophase stages of normal bone marrow cell mitosis, a marked reduction in the number and in the size of DNA helix openings was observed, correlating with the decreased rate of RNA synthesis occurring in these cells at these times. The euchromatin localization of these DNA helix openings correlates with the localization within euchromatin of de-repressor RNA and other DNA ligands (Nature 206, 680 (1965) known to favor the formation of DNA helix openings (Nature 208, 1093 (1965). Supported by Research Grants CA-10174 and CA-13524 from the National Cancer Institute, IC-45 from the American Cancer Society, and by a research scholar award from the Leukemia Society.

F-PM-E3 CHARACTERIZATION OF A CLASS OF HIGH DNA AFFINITY NHC-PROTEINS OF RAT LIVER, L. L. Jagodzinski,* J. C. Chilton,* J. S. Sevall, Chemistry Department, Texas Tech University, Lubbock, Texas 79409

Male rat liver nonhistone chromosomal (NHC)-proteins have been fractionated based on their affinity for phosphocellulose. A moderate binding fraction of NHC-proteins (12.1±5.8% of their total) was found to bind at physiological ionic strengths (250mM-500mM). Sodium dodecyl sulfate polyacrylamide gel electrophoresis indicated that a heterogeneous group of molecular weight polypeptide components were obtained. The DNA binding properties of the fractionated NHC-proteins were investigated by the membrane filter technique. Temperature had little effect on NHC-protein DNA interactions; whereas, increased ionic strengths profoundly affected the protein DNA complexes. At 300mM or 350mM ionic strengths, 22% of the total DNA which is enriched in repetitive sequences can be retained at saturation by the moderate binding NHC-proteins. The bound (B)DNA at 350mM ionic strength could be separated from the unbound (UB)DNA. Rentention of the B-DNA and UB-DNA on membrane filters with the moderate binding NHC-proteins resulted in 70-80% retention of the B-DNA sequences and less than 10% retention of the UB-DNA sequences. Fractionation of the moderate binding NHC-proteins over rat DNA cellulose at 350mM ionic strength indicated 1.3% of the total NHC-proteins represented by polypeptides of 23,000-18,000 daltons can interact with high affinity sites in rat DNA.

F-PM-E4 ON THE CHROMOSOMAL INTEGRATION OF DISPROPORTIONATELY REPLICATED RIBOSOMAL GENES IN DROSOPHILA MELANOGASTER. C. Zuchowski* and A. Gayler Harford, Division of Cell and Molecular Biology, State University of New York at Buffalo, Buffalo, N. Y. 14214.

The purpose of this investigation was to determine whether the ribosomal genes are integrated into chromosomal DNA or whether they exist as an extrachromosomal unit as proposed in models for the regulation of ribosomal gene multiplicity in Drosophila. We have analyzed by sucrose gradient sedimentation DNA from adult flies in which disproportionate replication of ribosomal genes is expected to occur, i.e. y w spl bb/Y^{-bb} (♂), g^2 ty bb/Y^{-bb} (♂), and y w spl bb/In(1) sc^{4L} sc^{8R}, y sc^4 sc^8 cv v B (♀). To minimize fragmentation of the DNA, the gentle lysis procedure of Kavenoff and Zimm (1973) was used, which has been shown to yield chromsome-sized DNA. The DNA of all three genotypes sedimented as a single peak. For y w spl bb/Y^{-bb} and g^2 ty bb/Y^{-bb} all of the ribosomal genes are present in this peak as shown by hybridizing fractions of the gradient with ribosomal RNA. Using T4 (1.2×10^8 daltons) and B. subtilis W23 (1 to 4 x 10^9 daltons) DNAs as markers, a molecular weight of 5 to 10 x 10^9 was estimated. In y w spl bb/In(1) sc^{4L} sc^{8R}, y sc^4 sc^8 cv v B about 68% of the ribosomal genes were found in this high molecular weight peak and 32% in a region of lower molecular weight ($\sim 4 \times 10^8$). These results demonstrate a significant difference in the physical state of the ribosomal genes in these genotypes. We suggest that the high molecular weight genes are integrated into the chromosome and the low molecular weight genes are present in extrachromosomal DNA. [Supported by NIH grant No. GM 21487 to one of us (AGH)].

F-PM-E5 CHARACTERIZATION OF NASCENT DNA THROUGH STUDIES OF THE INHIBITION OF INITIATION OF MAMMALIAN REPLICONS. M.R. Mattern*, L. Povirk*, B.R. Young* and R.B. Painter, Laboratory of Radiobiology, University of California, San Francisco, San Francisco, Calif. 94143

Inhibition of mammalian cell DNA synthesis by x-radiation is characterized by decreased amounts of low molecular weight DNA formed 30 minutes after the irradiation (100-1000 rads). This result shows that ionizing radiation inhibits initiation of DNA synthesis; there is no detectable effect at these doses on DNA chain elongation. The substitution of thymine residues in DNA by 5-BUdR and subsequent exposure of cell cultures to 313 nm wavelength light causes an identical pattern of inhibition of replicon initiation. It is likely therefore that the molecular target of replicon initiation is DNA itself and that inhibition occurs because damage anywhere within a cluster of replicons blocks initiation of all the replicons therein, suggesting that initiation depends in part upon the maintenance of some physical state of DNA within the cluster. When the nascent DNA formed during inhibition of initiation is examined by DNA-DNA hybridization (C_0t) techniques it is found to contain more sequences of intermediate repetition than does nascent DNA from control cells. This result will be discussed in terms of distribution of different classes of DNA within replicons.

F-PM-E6 CHANGES IN CHROMATIN ORGANIZATION DURING THE CELL CYCLE. C. E. Hildebrand, R. A. Walters, R. A. Tobey*, and L. R. Gurley*, Cellular and Molecular Biology Group, Los Alamos Scientific Laboratory, University of California, Los Alamos, New Mexico 87545, USA.

We have found that the natural polyanion, heparin, is a useful agent for measuring changes in chromatin organization. Heparin treatment of isolated nuclei causes rapid nuclear swelling and release of DNA from chromatin. The kinetics of nuclear swelling activated by heparin were measured as the rate of decrease in 600 nm absorbance of a suspension of nuclei, and the rate of DNA release from nuclei was determined by centrifugal separation of released DNA from DNA remaining condensed in chromatin at various times after addition of heparin to a nuclear suspension. These parameters were used to monitor changes in chromatin organization during the cell cycle. Synchronized populations of Chinese hamster cells (line CHO) were obtained by mitotic selection or isoleucine deprivation. In some experiments, early G_1 populations derived by these procedures were resynchronized near the G_1/S boundary by growth in hydroxyurea containing medium. In nuclei from early G_1 cells, heparin-mediated nuclear swelling and DNA release were observed to proceed at rates 2-3 fold greater than the rates for late G_1 nuclei. Because of its polyanionic character, heparin interacts primarily with the histone component of chromatin. Hence, our results suggest that as cells traverse the G_1-phase of the cell cycle, nuclear structure undergoes changes which either decrease the accessibility of histones to heparin or increase the affinity of histones for DNA. The possibility exists that the changes in chromatin organization observed using heparin and the G_1-specific phosphorylation of f1 are both related to a structural alteration in chromatin organization prior to the initiation of DNA synthesis. (This work was performed under the auspices of the U. S. Energy Research and Development Administration.)

F-PM-E7 UPTAKE OF LABELED PRECURSORS INTO NUCLEAR AND MITOCHONDRIAL DNA DURING DEVELOPMENT OF THE CELLULAR SLIME MOLD, DICTYOSTELIUM DISCOIDEUM. R.A. Deering, Department of Biochemistry and Biophysics, The Pennsylvania State University, University Park, PA 16802

Without nutrient, the cells of D. discoideum aggregate and develop with only limited cell division to yield fruiting bodies, with differentiated spore and stalk cells. The DNA is about 65% nuclear (n), mostly at a density of 1.676 (in CsCl), and 35% mitochondrial (m) of density 1.682. The uptake of ^{3}H-labeled thymidine (dT), deoxyadenosine (dA), and adenine(A) into the m- and n-DNA was measured at several developmental stages. Strain NC-4 was grown to stationary phase on E. coli B/r. These cells were washed and incubated in buffer for 9 hours and then deposited on MF filters. Aggregation began immediately. At several times, the developing cells were pulse labeled for 1.5 hours and lysed. Before CsCl banding, Netropsin was added to the lysates. This antibiotic preferentially attached to A-T and nearly doubled the separation of the m- and n-DNA in the gradients, greatly improving the quantitative resolution of the label in these bands. Although at a relatively low level of uptake, distinct patterns of labeling were observed. With dT or dA, only m-DNA was labeled during pulses at the end of aggregation; later, at pre-culmination, the n-DNA was preferentially labeled. Adenine uptake was preferentially into n-DNA at all stages when labeling occurred. BUdR present at >500 µg/ml produced only a slight density shift. FUdR up to 400 µg/ml did not diminish dT or dA uptake, nor block development. A small increase in cell number during development has been observed but it is not clear how this relates to the labeling. The interpretation of the patterns of uptake may be further complicated by possible changes in permeability and pools. (NIH GM-16620 and CA-01014)

F-PM-E8 TEMPORAL INDUCTION OF 6-THIOGUANINE AND OUABAIN RESISTANCE IN SYNCHRONOUS CHINESE HAMSTER CELLS BY 5-BROMODEOXYURIDINE. P. M. Aebersold* and H. J. Burki, Division of Medical Physics, University of California, Berkeley, California 94720.

Mutants resistant to 6-thioguanine were induced by 5-bromodeoxyuridine (BUdR) in synchronous Chinese hamster cells. The induction of mutants was a function of the time of incorporation of BUdR into DNA, showing a maximum early in the DNA synthesis period. Preliminary data shows that ouabain resistance is induced by BUdR maximally about one hour later in the DNA synthesis period. Since deficiency of hypoxanthine-guanine phosphoribosyltransferase (HGPRT) results in 6-thioguanine resistance and since certain alterations in the ($Na^{+}K^{+}$)-associated ATPase of the plasma membrane result in ouabain resistance, these data suggest that temporal sequences of gene replication can be demonstrated by BUdR mutagenesis of synchronized cells.

F-PM-E9 GENETIC AND COMPLEMENTATION OF MUTANTS OF HAEMOPHILUS INFLUENZAE DEFICIENT IN ATP-DEPENDENT NUCLEASE. J. K. Setlow, J. Kooistra*, G. D. Small*, and R. Shapanka*, Biology Department, Brookhaven National Laboratory, Upton, Long Island, New York 11973.

Eight different mutations in H. influenzae leading to deficiency in ATP-dependent nuclease have been investigated in strains in which the mutations of the originally mutagenized strains have been transferred into the wild type. Complementation between extracts and genetic crosses show that there are three complementation groups corresponding to three genetic linkage groups. Thus it is reasonable to postulate that there are three cistrons in H. influenzae that code for the three known subunits of the ATP-dependent nuclease. The wild type enzyme is known to have DNA-dependent ATP-ase activity associated with it. Half of the mutants show this activity. This group is also considerably more resistant to inactivation by deoxycholate and certain antibiotics than the other mutants. Three of the members of this group comprise one of the complementation-linkage groups. The other mutant with ATP-ase activity is in a linkage group with mutants sensitive to deoxycholate and lacking this activity. We conclude that ATP-ase activity is a property of the configuration of the enzyme, probably specified by only two of the three cistrons, and that lack of ATP-ase activity may be correlated with increased permeability of the cell. Research carried out at Brookhaven National Laboratory under the auspices of the U. S. Energy Research and Development Administration.

F-PM-E10 SEPARATE GENETIC CONTROL OF SEROTONIN STORAGE IN BLOOD PLATELETS AND BRAIN REGIONS OF THE MOUSE. E.Gfeller, J.M.Holland*, and D.A.Gfeller-Varga*,Psychiatry Service,VA Hospital Birmingham and University of Alabama in Birmingham, School of Medicine, Birmingham,Alabama 35294, and Biology Division, Oak Ridge National Laboratory, Oak Ridge,Tennessee 37830.

Beige mice (bg/bg) show a prolonged bleeding tendency, markedly decreased serotonin (5-HT) content in blood platelets, decreased adenine nucleotide levels in platelets, and impaired ^{3}H-5-HT uptake in vivo. We studied in vitro uptake of ^{3}H-5-HT in various brain regions into slices, and assayed endogenous 5-HT concentrations in the same brain regions. C57BL/6 mice of comparable age were used as controls. Neither in vitro uptake of ^{3}H-5-HT nor endogenous levels of 5-HT were different in the mutant as compared with the wild-type animals. Platelet 5-HT, therefore, does not reflect brain levels of 5-HT. Uptake and endogenous levels compared well with similar data from other species. The considerable behavioral differences between the two strains presumably are unrelated to the platelet defect, and may be another expression of the pleiotropy of the bg gene.

F-PM-E11 CYTOPLASMIC AND POLYSOME-DERIVED MESSENGER RIBONUCLEOPROTEIN PARTICLES IN CHICK EMBRYONIC MUSCLES. R. Coronado*, S.K. Jain*, J. Bag and S. Sarkar. Dept. Muscle Research, Boston Biomedical Res. Inst. and Dept. Neurology, Harvard Medical School, Boston, Mass. 02114.

Previously we reported the isolation of cytoplasmic non-polysomal messenger ribonucleoproteins (CmRNP) containing mRNAs coding for actin and myosin heavy chain from chick embryonic muscles by a combination of ultracentrifugation and sucrose density gradients (Biochem. 14, 3800, 1975). We have now used a simple method for further purification of mRNP particles by affinity chromatography on oligo-(dT) cellulose. When subribosomal or post-polysomal fractions of chick embryonic muscles are applied to oligo-(dT) cellulose columns, 1-2% of the uv-absorbing material is bound to the column. Elution with 50% formamide releases this material as a sharp single peak of CmRNP. Polysomal mRNP (PmRNP) can be purified from EDTA dissociated free polysomes using the same method. The mRNP fractions are identified by their characteristic buoyant density of 1.4 in CsCl gradients, by the absence of typical ribosomal proteins as shown by polyacrylamide gel electrophoresis in the presence of SDS and by the presence of poly-A in their RNA moieties. Upon SDS gel electrophoresis CmRNP particles show a complex protein pattern including seven protein bands in the 44,000-85,000 dalton range. The protein patterns of PmRNP are simpler than those of CmRNP. PmRNP contains two major bands of molecular weight 78,000 and 58,000 and a number of minor bands. The protein bands in the 44,000-50,000 dalton range present in CmRNP could not be detected in PmRNP. The significance of these results in relation to the possible role of CmRNP in translational control during myogenesis will be discussed. (Supported by grants from NIH AM-13238 and the Muscular Dystrophy Associations of America, Inc.)

F-PM-E12 GENOME EVOLUTION IN THE CRUSTACEA. J.C. Vaughn and F.J. Traeger*, Department of Zoology, Miami University, Oxford, Ohio 45056.

Analysis of data obtained from molecular hybridization of ^{3}H-labeled repetitious DNA has been utilized to reconstruct the broad outlines of phylogenetic relationships among decapod Crustacea. This molecular reconstruction agrees with the paleontological record, and with other schemes obtained by comparative morphological and serological approaches. Preliminary data derived from analysis of hybrid thermal stability profiles and also from cot kinetics of species having different genome sizes is in line with the hypothesis that continuous addition of new repeated sequence families to the genome over long periods of time may in part account for the correlation observed between percent repeated DNA hybridized and divergence time. Calculation of the rate of addition of repeated DNA sequences to the genome suggests that for relatively recently diverged species the rate is about 0.7% total genome growth per 10^{6} yr. This is comparable to the rate for mammalian (rodent) genomes [Kohne, Quart. Rev. Biophys. 3, 327 (1970)]. Thermal stability analyses of hybrids leads to the tentative conclusion that a core of repeated DNA base sequence homology has been highly conserved throughout the evolution of the Crustacea. Demonstration of inter-species sequence homology has important implications to models which relegate a genetic regulatory function to repeated DNAs. (Supported by NSF grant GB-29486, grant 6088 from the Penrose Fund of The American Philosophical Society, and by faculty research grants from Miami University).

F-PM-E13 THE EVOLUTION OF EUKARYOTE ORGANELLES INFERRED FROM PROTEIN AND NUCLEIC ACID SEQUENCES. R.M. Schwartz and M.O. Dayhoff, National Biomedical Research Foundation, Georgetown University Medical Center, 3900 Reservoir Road, NW, Washington, D.C. 20007

The divergence of the eukaryotes from the prokaryotes (perhaps 1.4 billion years ago) produced a sharp discontinuity in cellular organization and structure. Recently, considerable attention has focused on the idea that eukaryotes arose from prokaryotes through a series of symbiotic associations between a large host cell and various kinds of smaller cells which have become eukaryote organelles. Several groups of known protein and nucleic acid sequences are sufficiently ancient and well conserved to reflect the required prokaryote divergences; for example, cytoplasmic 5S ribosomal RNA sequences reflect the divergence of the eukaryote host from bacteria and blue-green algae. Evolutionary trees based on ferredoxin, plastocyanin-azurin, and c-type cytochrome sequences provide evidence for the endosymbiotic origin of chloroplasts. Plant ferredoxin, plastocyanin, and cytochrome c_6 are all functional components of the photosynthetic apparatus of the chloroplast or photosynthetic lamellae (in blue-green algae) and have been sequenced from blue-green algae and higher plants. Related sequences such as bacterial ferredoxins, cytochromes, and azurins provide both a time orientation and scale for these trees. Complete sequences from 11 families of c-type cytochromes also provide a context for understanding the evolution of eukaryote mitochondrial cytochrome c. The evolutionary tree of these proteins sheds light on the identities of the prokaryotes involved in the origin of the mitochondrion. *Supported by NASA contract NASW-2848 and NIH Grant GM-08710.*

F-PM-F1 A MODEL OF THE CHANGES IN SOME TISSUE COMPONENTS FOLLOWING INFARCTION. Richard P. Spencer, Larry A. Spitznagle.* Department of Nuclear Medicine, University of Connecticut Health Center, Farmington, Connecticut, 06032.

Following interruption of the oxygen supply to tissues, most frequently via acute arterial blockade, complex events occur in the systems for synthesizing and degrading biochemical components, as well as in the permeability of the area. A first approach to analyzing the situation was made by utilizing a simple model. Any substance in the infarcted area might be reduced in amount by means of decreased production and increased loss or destruction. The loss can be either into surrounding tissues or into the blood stream. To permit an initial quantitative approach, we have utilized data on nicotinamide coenzymes in the dog heart (Nunez at al, Am. J. Physiol. 226:73, 1974). A decrease occurs in the nicotinamide coenzyme NAD, within cardiac muscle, during the course of myocardial infarction in dogs. The amount (A) at any time, minus a basal level (B, in nmol/g) can be expressed as a single exponential: $A - B = Ce^{-0.23t}$ (where t is in hours). The same rate constant also appears to hold for the decrease in myocardial $NADH_2$. Of the NAD lost from the infarcted myocardium, some may be found in the blood stream at 2 hours (at least the blood level shows a minor rise). Simple analogue computer models have been constructed of the events. (Supported by USPHS CA 17802 and by American Cancer Society DT-34E).

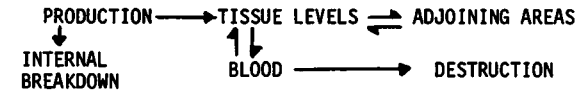

F-PM-F2 COUPLING OF EXERGONIC AND ENDERGONIC REACTIONS AND THE EFFICIENCY OF ENERGY TRANSDUCTION IN BIOLOGICAL SYSTEMS. Ljubiša Vitković, Departments of Biophysics and Microbiology and Public Health, Michigan State University, E. Lansing, MI 48824

Mechanisms of energy transduction in biological systems remain as one of the fundamental unsolved problems of bioenergetics. Information about energy transduction in mitochondria is utilized for deduction of two kinds of couplings of exergonic and endergonic reactions. The failure of experimentalists to identify and isolate " high-energy" intermediate, which supposedly couples electron transport and oxidative phosphorylation, is rationalized on this basis. Efficiency of energetic processes emerges from the analysis as an important experimental and theoretical parameter. It is proposed that the efficiency of coupling is optimal for a given system under a given set of conditions. The optimal efficiancy results from the sensitively balanced relationship between the magnitude of energy to be transduced and the number of the degrees of freedom employed in the transduction.

This work was supported in part by the funds from the College of Osteopathic Medicine, Michigan State University and the Yugoslav (Serbian) Community for Scientific Work.

F-PM-F3 NUCLEAR MAGNETIC RESONANCE PATTERNS OF CELLULAR WATER IN SYNCHRONIZED HELA CELLS. C. F. Hazlewood, P. T. Beall‡ and P. N. Rao‡ Department of Pediatrics, Baylor College of Medicine and Department of Developmental Therapeutics, The University of Texas System Cancer Center M. D. Anderson Hospital Tumor Institute, Houston, Texas.

Pulsed nuclear magnetic resonance (NMR) relaxation times (T_1 and T_2) of intracellular water protons were measured in HeLa cells synchronized in various phases of the cell cycle. The percentage of water was also measured in each phase of the cell cycle. Random populations of HeLa cells have a T_1 of 667 m sec and T_2 of 112 m sec. The T_1 values for mitosis, G1, S and G2 were 1020, 650, 534 and 621 m sec respectively, Mitotic cells collected either by colcemid or N_2O block have identical T_1 values. If the T_1 of mitotic cells (collected after the release of N_2O block) is taken as 100%, then within 30 min of incubation under normal culture conditions the T_1 drops to 80% and by 4 hrs (G1) to 60%. The T_1 value reaches the lowest level (52%) in S phase cells and then rises as the cells progress through G2 thus reaching its peak once again in mitosis. In general the T_2 values follow a similar pattern. The water content and the relaxation times are proportional in the transition from M to S; however, between S and G2 the relaxation times are independent of hydration. Condensation of chromatin of S phase cells with spermine resulted in an uncoupling of the hydration effect from the relaxation phenomenon. This study indicates that the physical state of cellular macromolecules play an important role in determining the relaxation times of water hydrogens. (Supported in part by R. A. Welch Foundation, NIH Grants and Contracts CA-16480, CB-43978; GM-20154, RR-0188, and the Office of Naval Research N0014-75A).

F-PM-F4 CALORIMETRIC ASSESSMENT OF THE ACTIVITY OF LYMPHOCYTES UNDER MITOGENIC STIMULATION. T. Lee* and H. Krakauer, Program in Biochemistry and Biophysics, Washington State University, Pullman, WA. 99163.

The overall metabolic activity of equine lymphocytes obtained from animals that had been subjected to prolonged immunization was assessed by calorimetric measurement as a function of incubation time in the absence of mitogens and in the presence of the lectin mitogen concanavalin A (con A) or of the specific immunizing agent, dinitrophenylated bovine serum albumin (DNP-BSA). Heat is evolved by freshly isolated lymphocytes at a rate of up to 1,200 μcal/min/10^7 cells. Upon incubation in L-15 (Leibowitz) medium supplemented with 20% horse serum, at 37°C, heat output decays progressively over 72-96 hrs to about 40 μcal/min/10^7 cells without appreciable deterioration in cell viability. Such lymphocytes, when incubated in the presence of con A or DNP-BSA, are stimulated to proliferation, with an efficiency by the latter of 20% of the former when determined by measurement of DNA synthesis. Both agents display maximal effects in that assay after 72 hours of exposure. Cells exposed to con A evolve heat at elevated rates: 1.5 fold higher than controls after 6 hrs, 2-fold higher after 24 hrs and about 5-fold higher after 48 and 72 hrs of exposure. In contrast, lymphocytes from the same immunized animal fail to exhibit elevations of heat output after exposures of up to 48 hrs to DNP-BSA in measurements in which effects of 5-10% of the magnitude of those due to con A are readily detectable. Only after 72 hrs is the expected elevation of heat output observed. These data suggest that the processes of lymphocyte activation by the specific stimulant DNP-BSA and the non-specific mitogen con A differ at the level of metabolic organization of the cell.

F-PM-F5 CHRONIC GRANULOCYTIC LEUKEMIA: A DISEASE OF ALTERED SHORT RANGE CONTROL AT THE PLURIPOTENTIAL STEM CELL LEVEL? Michael C. Mackey, Departments of Physiology and Biomedical Engineering, McGill University, Montreal, CANADA.

In normals, the granulopoiesis control system functions to produce either a constant or mildly oscillating level of circulating granulocytes. Although details are missing, the bread outlines of the humoral feedback mechanisms involved in the control of granulopoiesis are understood. Chronic granulocytic leukemia is a disease of the granulocyte series characterized by widely fluctuating levels of circulating granulocytes that may be either periodic or aperiodic. There is indirect evidence that the defect is resident in the short range control mechanisms operating at the pluripotential stem cell level. A simple discrete time model for the short range control of the pluripotential stem cells, based on reasonable physiological mechanisms, has been examined. In the simplest form of the model all of the stem cells are assumed to be in a proliferating state and evolving according to the dynamical equation $P(i+1)=2\alpha(i)P(i)$, where $P(i)$ is the population during the ith generation time, $\alpha(i)$ is the fraction of cells re-entering proliferation during the ith generation time, and 2 accounts for mitosis. In accord with existing data, it is assumed that $\alpha(i)=1/(1+P^n(i))$, where n is the only adjustable parameter. It is found that with small alterations in the control dynamics (changes in n) the model passes from one globally stable steady state, through stable limit cycles of various periods, to an apparently random fluctuation in the $P(i)$. This behaviour, and the similar behaviour of a more realistic model including a pool of non-proliferating cells, will be discussed.

F-PM-F6 ESTIMATION OF RHYTHM PARAMETERS FROM SINGLE CYCLES OF A TIME SERIES. N. W. Hetherington*, L. S. Rosenblatt*, and C. W. Winget. Geneticon, 1111 Oakland Avenue, Piedmont, CA 94611, and NASA, Ames Research Center, Moffett Field, CA 94035.

In the analysis of time series data by utilization of Fourier series, the assumption is implicit that the data are stationary in time. In particular, it is assumed that the period is invariant through the time series. Present methods of estimation of the period, e.g., periodogram analysis, require the same assumption. In biology where the data often are not extensive and where there are reasons to suspect that the period may be changing with time, current methods of period estimation are invalid. Our interest in this problem arose from a need to define the trajectory of the period as it reaches a new steady state following a change from a L:D to L:L photoperiod. We present a method which permits the simultaneous estimation of the period, phase angle, mean and amplitude without the necessity of making any assumptions, while utilizing short segments of the data. In fact, it should be possible to utilize only single cycles of the data, thus obtaining the dynamics of the change in period. The mathematical method consists of the development of four simultaneous linear equations on four unknowns. The period, phase angle, mean and amplitude are shown to be functions of the four coefficients estimated from the data. The period is observed to be the only independent parameter in that the phase angle, mean and amplitude are functions of the period. Thus, it is not possible to alter the phase angle, mean or amplitude without altering the period. The applicability of the mathematical model to biological data will be discussed.

F-PM-F7 DYNAMICAL MODEL FOR PATTERN FORMATION IN DEVELOPMENT. K. Trabert, Laboratory of Theoretical Biology, DCBD, National Cancer Institute, National Institutes of Health, Bethesda, Maryland 20014, and S.A. Kauffman, Department of Biochemistry and Biophysics, University of Pennsylvania, Philadelphia, Pennsylvania 19104.

A reaction diffusion model is proposed for the purpose of qualitatively explaining developmental phenomena such as, pattern formation, regeneration, duplication, and supernumerary limb regeneration in the wing disk of Drosophila melanogaster and other epimorphic fields. In this model each cell in the developmental field knows his unique location through the growth of a definite spatial pattern of morphogens which arises after the tissue imbedding the field has grown to a given critical size. Axes of symmetry and compartments of development which have been observed experimentally are created by the model as time increases. Computer simulation shows the model accounts for a range of regenerative and duplicative phenomena already observed for the wing disk of Drosophila melanogaster and makes further predictions which are accessible to experimental testing.

F-PM-F8 PRELIMINARY ESTIMATES OF THE PERMEABILITY OF MOUSE OVA AND EARLY EMBRYOS TO GLYCEROL. Peter Mazur, N. Rigopoulos*, S. C. Jackowski*[1], and S. P. Leibo*. Biol. Div., Oak Ridge Natl. Lab., and UT-Oak Ridge Grad. Sch. Biomed. Sci., Oak Ridge, Tenn. 37830

The permeability of ova and early embryos to solutes is of physiological significance, and it is central to understanding their response to subzero temperatures. The present study is concerned with determining the permeability coefficient for glycerol and its temperature dependence. Coefficients were calculated from measurements of cell volume versus time in 1 M glycerol at 0°, 15°, or 22° for unfertilized ova and for 1-, 2-, 4-, and 8-cell embryos. Ova and embryos were transferred to 1 M glycerol in saline and photographed during the ensuing shrinkage and swelling. Volumes were estimated from planimetric measurements of the cross-sectional area, assuming the ova and embryos to be spherical. The increase in cell volume with time is described by two coupled equations (Mazur et al., J. Memb. Biol. 15:107, 1974). One expresses continuous osmotic equilibrium between the intra- and extracellular solution. The other relates the rate of glycerol entry to the difference in the concentration of intra- and extracellular glycerol. Permeability coefficients (P) were calculated by determining the numerical value of P required in the latter equation to make the calculated volume equal to the observed volume at a selected time. Calculated and observed plots of volume over the whole time course of permeation agreed satisfactorily. Fertilization produced about a 3-fold increase in P. Further development from the 1-cell to the 8-cell stage produced an additional 10-fold increase in P from $\sim 3 \times 10^{-5}$ to $\sim 3 \times 10^{-4}$ cm/min at 22°C. The value of P for 2-cell embryos at 3°C was about 10-fold lower than the value at 22°C. The permeability of the 8-cell embryo to glycerol at 22°C is comparable to that of the human red cell. (Research sponsored by Energy Res. and Development Adm. under contract with Union Carbide Corp. [1]Predoctoral Fellow supported by grant GM1974 from NIGMS, NIH.)

F-PM-F9 CHEMICALLY DIFFERENTIATED STATES OF A LINEAR ARRAY OF CELLS WITH ENZYME-CATALYZED REACTION. Barry Bunow, Division of Computer Research and Technology, Laboratory of Applied Studies, National Institutes of Health, Bethesda, Md. 20014

In development, a group of embryonic cells which are similar initially differentiates into distinguishable progeny. While the biochemical basis for this process is still obscure it is clear that communication between cells is a part of the story. As a simple model, a linear array of identical cells, in diffusional contact with their neighbors in the array and with a nutrient reservoir is considered. Each cell contains the same concentration of an enzyme catalyzing a reaction involving the externally supplied substrate and obeying substrate inhibition kinetics. The material balance equations for this system contain three essential parameters: the Thiele modulus, the Biot number, and the ratio of external substrate concentration to the K_M of the enzyme. For certain values of these parameters, there are a great many distinct stationary states--as many as 3^N of which 2^N are stable (N being the number of cells). The character of these states is diverse, there being uniform concentration profiles, ones with gradients down the array, and ones with multiple maxima and minima in concentration. Numerical studies have been made to show the variation of the number and character of the states with the problem parameters. To reconnect these results with the development problem, it might be expected that cells with different concentrations internally would induce different enzyme patterns; but this aspect is beyond the scope of the present model.

F-PM-F10 BIOPHYSICAL PROPERTIES OF RENAL EXCITABLE MEMBRANE. C.E. Constantinou, Department of Surgery (Urology), Stanford University School of Medicine, Stanford, Calif. 94305

The nonlinear oscillator properties of the excitable tissues of the renal pelvis are presented in terms of a physical-chemical system of membrane oscillators. The spectra of oscillations exhibited by this system are formulated on the basis of structural observations at various sites of the calyceal system. Experimental evidence is provided to demonstrate that a multiple system of independent oscillators are closely coupled by hydrostatic pressure to produce a conducted action potential. The mathematical description in terms of the theoretical equations of this nonlinear oscillation system is presented qualitatively and illustrated graphically. The morphological analogue of these concepts are shown in a short 2.5 minute film.

F-PM-F11 PHYSICAL CONDITIONS FOR COUPLING RATE-DEPENDENT AND RATE-INDEPENDENT MORPHOGENESIS. H. H. Pattee, School of Advanced Technology, State University of New York at Binghamton, Binghamton, N.Y. 13901.

Morphogenetic events may be distinguished as rate-dependent, dynamical growth or as rate-independent, syntactic growth. For example, the synthesis of proteins is primarily a sequential process that does not depend crucially on the rate of transcription or translation. The self-assembly of virus particles and many types of cell-sorting are also rate-independent growth processes. On the other hand, most cell morphologies depend on differential rates of growth of their macromolecular components, and most multicellular organisms have morphologies that emerge from differential growth rates of their differentiated cell lines. What are the physical conditions that permit the coordination of rate-dependent and rate-independent growth? It is reasonable to associate simple rate-independence with either minimum energy or maximum probability equilibrium configurations. It is also reasonable to associate the rate of an event with the activation energies leading to that event. Thus the enzyme is a localized, non-integrable constraint that couples a rate-independent specificity with a rate-dependent catalysis. However, dynamic-syntactic couplings in morphogenesis also depend on delocalized, but coherent sets of constraints that have no simple embodiment. Waddington speaks of these coherent sets as chreods, and Thom represents them abstractly in his catastrophe theory; but the physical conditions for such constraints require consideration of reliability, error propagation and hereditary selection processes that are closer to biological observables.

F-PM-F12 SIMULATION OF FOOT-AND-MOUTH DISEASE VIRUS NEUTRALIZATION. R. Trautman, Plum Island Animal Disease Center, P.O. Box 848, Greenport, New York 11944

For the small spherical animal viruses, at least, there is considerable controversy concerning in-vitro antigen (Ag) - antibody (Ab) reactions. Paradoxes have arisen primarily because virologists have designed tests for a specific (usually diagnostic) purpose rather than for revealing the mechanism of the reaction in depth. It is the purpose of this paper to present yet another manner of plotting checkerboard neutralization data that gives a map of the entire reaction. The ordinate is the fraction of infectious virus remaining and the abscissa is the initial concentration ratio of virus to antiserum, both coordinates on a log scale. Data or interpolated points are connected for three types of test protocols: 1) constant Ag (variable antibody "plaque reduction" assay), 2) constant Ab (variable antigen "virus neutralization index" assay), and 3) constant indicator Ag (block "quantal endpoint" assay). Simulation on a digital computer of equilibrium mass action relationships revealed the maps expected under a variety of circumstances. From such theoretical patterns, deductions can be made concerning the: 1) relationship between neutralization valence and the total Ag valence, 2) effect of non-infectious virus on the reaction, 3) changes caused by monogamous bivalent Ab binding, 4) influence of heterogeneity of reagents, 5) similarity between radioimmune and virus neutralization assays, 6) procedures for computing intrinsic equilibrium constants, 7) relationships anticipated in neutralization kinetic studies, and 8) logical extension to a fourth test protocol of constant indicator Ab (labelled Ab block radioimmune or "equilibrium filtration" assays).

F-PM-F13 THERMAL DENATURATION AT BODY TEMPERATURE: A POSSIBLE DETERMINANT OF PROTEIN TURNOVER RATES. Horton A. Johnson, Department of Pathology, Tulane University School of Medicine, New Orleans, La. 70112

The rates of inactivation of respiration of mouse liver slices were measured at temperatures from 41 to 46° C. The inactivation rates were strongly temperature dependent and followed the Arrhenius law. The effective activation energy of this process was 119 kcal/mole, indicating that the rate-limiting step in the thermal inactivation of cellular respiration involves the denaturation of a protein, probably a respiratory enzyme. By extrapolating the Arrhenius plot, it was possible to estimate the rate at which the essential protein would be denatured at normal body temperature. This extrapolation showed that at 38-39°C, the *in vivo* temperature of the mouse liver, the half-life of this protein is limited to only 10-20 hours due to thermal denaturation. The very rapid *in vivo* turnover rates of certain liver enzymes has never been adequately explained. The present data suggest that these fast turnover rates may simply represent the maintenance of a steady state in the presence of thermal noise.

F-PM-F14 *IN VITRO* AFLATOXIN B_1 METABOLISM BY HUMAN LIVER ACROSS INDIVIDUALS. D.M. Yourtee* and D.L. Phillips* (intr. by G.J. Bartling), Biochemistry Department, Cancer Research Center, Columbia, Missouri 65201

Aflatoxin B_1 was metabolized *in vitro* by liver homogenates from six cancer patients of varying sex, age, and liver status, to elucidate overall patterns of metabolism by humans, and the effect on these patterns of compounds known to affect aflatoxin toxicity in animals. Aflatoxin M_1 was a consistent metabolite produced in small amounts; aflatoxin Q_1, aflatoxicol and aflatoxicol H_1 were not always observed, but were at times major metabolites; the latter two metabolites were never found together in the same specimen. Primary liver histopathology did not appear to exert predominant influence on product patterns; however, reductive pathways were favored with partially inactivated tissue. Nicotinamide inhibited overall metabolism, and in addition caused a shift to reductive metabolites; methionine had a slight promotive effect, and favored oxidative products. One of the biopsy specimens was found to contain the toxin, apparently environmentally ingested, to the extent of 524 ng/g of wet liver. No other metabolites were detected, but upon incubation of a portion of the liver homogenate with an NADPH-generating system, the amount of Aflatoxin B_1 in the liver chloroform-extractable fraction was reduced to 250 ng/g, and another metabolite of higher polarity was observed, to the extent of 40 ng/g.